KARADENIZ TECHNICAL UNIVERSITY

THE GRADUATE SCHOOL OF NATURAL AND APPLIED SCIENCES

FOREST ENGINEERING   DEPARTMENT

MODELLING TIMBER VOLUME AND OTHER FOREST PARAMETERS USING LIDAR AND

FIELD DATA: A CASE STUDY FOR PART OF BERGAMA STATE FOREST ENTERPRISE

MASTER THESIS

Kennedy KANJA

JUNE 2016

TRABZON

KARADENIZ TECHNICAL UNIVERSITY
THE GRADUATE SCHOOL OF NATURAL AND APPLIED SCIENCES

FOREST ENGINEERING   DEPARTMENT

MODELLING TIMBER VOLUME AND OTHER FOREST PARAMETERS USING LIDAR AND FIELD DATA: A CASE STUDY IN BERGAMA STATE FOREST ENTERPRISE

Kennedy KANJA

This thesis is accepted to give the degree of
"MASTER   OF SCIENCE"
By
The Graduate School of Natural and Applied Sciences at
Karadeniz Technical University

The Date of Submission   **:** 01 / 06/2016
The Date of Examination   **:** 29/ 06 /2016

Thesis Supervisor   : Asst. Prof. Dr. Uzay KARAHALIL

Trabzon 2016

KARADENIZ TECHNICAL UNIVERSITY

THE GRADUATE SCHOOL OF NATURAL AND APPLIED SCIENCES

FOREST ENGINEERING DEPARTMENT

Kennedy KANJA

MODELLING STANDING TIMBER VOLUME AND OTHER SELECTED FOREST PARAMETERS USING LIDAR AND FOREST FIELD INVENTORY DATA: A CASE STUDY IN BERGAMA STATE FOREST ENTERPRISE

Has been accepted as a thesis of

MASTER OF SCIENCE

after the Examination by the Jury Assigned by the Administrative Board of the Graduate School of Natural and Applied Sciences With the Decision Number 1656 dated 07/06/2016.

Approved By

Supervisor : Asst. Prof. Dr. Uzay KARAHALIL ....

Member : Prof. Dr. Emin Zeki BAŞKENT ....

Member : Prof. Dr. İbrahim ÖZDEMİR ....

Prof. Dr. Sadettin KORKMAZ

Director of Graduate School

ACKNOWLEDGEMENTS

THESIS STATEMENT

I hereby declare that all the information contained in this master thesis titled 'Modelling timber volume and other forest parameters using LiDAR and field data; A case study for part of Bergama State Forest Enterprise' is as a result of my works under the supervision of Ass. Prof. Dr. Uzay KARAHALİL and with accordance with academic rules and ethical conduct. I also declare that, as required by these rules and conduct, I have fully acknowledged and cited all the material and results that are not originating directly from this work. 29/06/2016

Kennedy KANJA

TABLE OF CONTENTS

Master Thesis

SUMMARY

MODELLING TIMBER VOLUME AND OTHER FOREST PARAMETERS USING LIDAR AND FIELD DATA: A CASE STUDY FOR PART OF BERGAMA STATE FOREST ENTERPRİSE

Kennedy KANJA

Karadeniz Technical University
The Graduate School of Natural and Applied Sciences
Forest Engineering Department
Supervisor: Asst. Prof. Dr. Uzay KARAHALIL
2016, 79 Pages.

One of the biggest challenges in forest ecosystem planning is the measurement of forest inventories. Traditional methods of field measurements usually take time and costs lots of money. With the latest developments in remote sensing, precise estimation of some key forest parameters is becoming a reality. One of the new technologies that is being used for this is light detection and ranging (LiDAR). In this study, LiDAR derived tree height metrics as well as canopy density metrics as independent variables were regressed against the volume per ha, mean height, dominant height and number of trees per ha as dependent variables using SPSS and Excel. A total of 40 sample plots dominantly composed of *Pinus brutia* (Turkish red pine) were used. After processing the LIDAR data, a canopy height model (CHM) and canopy density model were obtained from which height and density metrics were derived respectively for the 40 sample plots. The best regression models obtained using LiDAR data alone had adjusted coefficient of determinations (R^2) of 0.66, 0.73, 0.83 and 0.83 for volume per ha, trees per ha, average height and dominant height and RMSE of 38.39 m^3 ha^{-1}, 109 trees ha^{-1}, 1.68 m and 1.78 m respectively. After integrating LiDAR and WorldView-3, the best adjusted R^2 was 0.70 for volume per ha and RMSE of 28 m^3 ha^{-1}. All the results were significant at 0.05 and thus credible.

Key Words: Forest stand parameters, Remote sensing, LiDAR, Tree Height, Bergama State Forest Enterprise, Worldview-3

Yüksek Lisans Tezi

ÖZET

LiDAR VERİLERİ VE YERSEL ÖLÇÜMLER YARDIMIYLA MEŞCERE HACİM VE BAZI PARAMETRELERİNİN MODELLENMESİ: BERGAMA ORMAN İŞLETME MÜDÜRLÜĞÜ ÖRNEĞİ

Kennedy KANJA

Karadeniz Teknik Üniversitesi
Fen Bilimleri Enstitüsü
Orman Mühendisliği Anabilim Dalı
Danışman: Yrd. Doç. Dr. Uzay KARAHALIL
2016, 79 Sayfa.

Orman ekosistemlerinin planlanmasında envanter aşaması, en fazla emek ve kaynağın harcandığı süreç olarak karşımıza çıkmaktadır. Özellikle son yıllarda teknolojide meydana gelen gelişmelere bağlı olarak, farklı uzaktan algılama tekniklerinin özellikle ağaç serveti envanterinde sıkça kullanılmaya başlandığı görülmektedir. Bu teknolojilerden birisi de LİDAR'dır. Dünya'da 1960'lı yıllardan itibaren kullanılan LİDAR verileri, orman envanterinde özellikle uydu görüntüleri ile birlikte kullanılmaktadır. Bağımsız değişkenler olarak ağaç boyu yükseklik, ve tepe yoğunluğunun bağımlı değişken olarak ise ağaç sayısı, üst boy, meşcere orta boyu ve hacmin dikkate alındığı bu çalışmada, saf Kızılçam (*Pinus brutia*) meşcerelerinden alınan 40 örnek örnekleme alanı verisinden hareketle SPPSS ve Excel yardımıyla farklı regresyon modeller geliştirilmiştir. LIDAR verileri işledikten sonra öncelikle tepe yüksekliği modeli (CHM) ve yoğunluğu farklı 40 örnek alan için elde edilmiştir. Sonrasında, örnekleme alanında yapılan ölçümler, geliştirilen indeksler ile ilişkiye getirilerek hektardaki hacim, meşcere orta boyu, üst boy ve hektardaki ağaç sayısı elde edilmiştir. Elde edilen en iyi regresyon modelleri; hektardaki hacim, hektardaki ağaç sayısı, meşcere orta boyu ve üst boy için sırasıyla 0.66, 0.73, 0.83 ve 0.83 düzeltilmiş R^2 verirken, yine sırasıyla 38.39 m^3 ha^{-1}, 109 ağaç ha^{-1}, 1.68 m ve 1.78 m RMSE elde edilmiştir. LİDAR verileri WorldView-3 uydu görüntüleri ile entegre edildikten sonra ise en iyi 0.70 R^2'ye ve 28 m^3 ha^{-1} hataya sahip hacim modelleri elde edilmiştir. Sonuçlar 0.05 anlamlı ve dolayısıyla güvenilirdir.

Anahtar Kelimeler: Meşcere parametreleri, Uzaktan Algılama, LİDAR, Ağaç Boy, Bergama, Worldview-3

LIST OF FIGURES

LIST OF TABLES

ABREVIATIONS

AGB   : Above Ground Biomass

ALS   : Air Borne Laser Scanning

ANOVA : Analysis of Variance

CHM   : Canopy Height Model

CW   : Continuous Wave

DBH   : Diameter at Breast Height

DEM   : Digital Elevation Model

DTM   : Digital Terrain Model

EMS   : Electro Magnetic Spectrum

GIS   : Geographical Information Systems

GPS   : Global Positioning System

LiDAR   : Light Detection and Ranging

LIF   : Laser-Induced Fluorescence

NS   : Number of Stems

R   : Coefficient of Correlation

R^2 : Coefficient of Determination

R_{cv}^2 : Cross-validated R^2

RMSE   : Root Mean Square Error

SPSS   : Statistical Package for Social Sciences

SV   : Stem Volume

SWIR   : Short Wave Infrared

VIF   : Variance Inflation Factor

VNIR   : Visible Near Infrared

1. GENERAL INFORMATION

1.1. Introduction

For as long as people have thought about the future they have managed forests. (Davies, 2001). Services provided by forests cover a wide range of ecological, political, economic, social and cultural considerations and processes (URL-1, 2016). The importance of forest management cannot therefore be over emphasized. In practical forestry, accurate information about growing stock and stand characteristics are crucial for successful forest management and planning. The forest management planning process starts with forest inventory. Also the estimation of forest aboveground biomass (AGB), which has received increasing attention during the last decade due to its relevance to global carbon cycle modeling and to international programs aimed at reducing greenhouse gas emissions, uses these inventory data (Laurin et al., 2014).

Forestry inventory data can be obtained from either remotely sensed data or from field survey with temporary sample plots and/or from the combination of both remotely sensed data and field survey as has been the case recently. Obtaining measurements of these parameters is costly and time consuming. Remote sensing techniques have been widely used for the estimation of some forest parameters especially since the beginning of new millennium. Those studies generally have used spectral information from satellite imagery such as Landsat, Spot, Aster or MODIS to model stand parameters over large areas (Günlü et al., 2013).

Naseri (2003), Khorramo (2004) and Mohammadi et al. (2007) used Landsat TM/ETM+ satellite images to model stand volume, density crown closure using regression models. For example Mohammadi et al. (2007) got R^2 of 43% for volume with error of 97.49 m^3 ha^{-1} and a R^2 of 73% for number of trees (density) with error of 170 trees per ha. Astola et al. (2004) using high-resolution satellite images to estimate forest stand parameters developed a decision support system. The developed Forestime software used the terrestrial measurements and satellite images to estimate the forest stand parameters. The following

RMSEs in percentage were obtained; 37.4% for volume, 23.4% for mean diameter and 87% for number of trees.

Other similar studies to estimate forest stand parameters using Landsat-TM/ETM satellite images include; Franco-Lopez et al. (2001), Makela and Pekkarinen (2004) and Kajisa et al, (2008). Also Reese et al. (2002) and Holmström et al. (2002) used SPOT satellite images to estimate some forest stand parameters.

Özkan (2003), used regression analysis to estimate forest stand parameters (number of trees, tree volume, basal area, average diameter and average height) using SPOT-5 image. Index values of bands 3 and 4 of SPOT-5 image were used to develop regression relationships with forest stand parameters while reflectance values were used for number of trees. Using the highest NDVI index gave R^2 of 0.26. Higher values ($R^2 > 0.5$) were obtained when using reflectance values from bands 2, 3 and 4 and PCI indexes to model tree volume with R^2s of 0.50, 0.51, 0.55 and 0.57. For basal area, of the three bands only band 4 indicated a higher relationship giving R^2 of 0.63. The study concluded that band 4 of SPOT-5 satellite image is the most sensitive to tree volume and basal area.

İnan (2004) used Landsat TM and ETM+ and inventory data to find regression relationships. His findings were that ETM5 band showed a strong relationship with all the forest parameters considered. With influence of different environmental conditions TK1 (Tasseled diameter algorithm luminance component), PC1 (principal components analysis 1 component), linear band combinations such as albedo and MID57, stand parameters with very strong statistical relationship ($R \geq 0.8$) were found.

Özdemir and Mert (2007) found a correlation coefficient of 0.40 for volume per ha after conducting a regression analysis between Quickbird (pan-sharpened) satellite data and terrestrial data for red pine stands of same age and with single-storey.

Ateşoğlu (2009), used 41 sample plots to develop regression models of forest parameters using Landsat 7 ETM+, SPOT HR-VIR, ASTER (VNIR) satellite images' band and vegetation indexes. For Landsat image data, diameter as dependent variable explained 24% variation while variation in basal area was explained by vegetation indexes (62%) and ETM bands (78%) respectively. ETMtk2, ETM4, ETMalbedo, ETMndvi explained 78% variation in basal area despite the low correlation coefficients with ETM4 and NDVI

variables. In the same way, variation in number of trees was explained by ETM (32%) and volume was explained by ETMtk2 (52%). Variation in number of trees when using SPOT image was explained by SPOT3 (12%). Likewise, variation in crown closure was explained by SAVI and Surface Alberdo (58%). For ASTER satellite image, variation in crown closure if explained by Aster3 variable alone was 49% while with addition of Asteralberdo and Aster2 was 66%.

Özdemir and Karnieli (2011) used WorldView-2 multispectral imagery for dry land forest in Israel with determination coefficient (R^2) and root mean square error (RMSE) values of the best fitting models, respectively, of 0.38 and 109.56 ha^{-1} for the number of trees (NT); 0.54 and 1.79 m^{2}ha^{-1} for the basal area (BA); 0.42 and 27.18 m^3 ha^{-1} for the stem volume (SV); and 0.67 and 0.70 for the standard deviation od diameters at breast height.

Günlü et al. (2013), tried Quickbird and Landsat 7 ETM+ satellite images and 70 sample plots to establish regression models for volume per ha in pure beech stands. The results of this study gave R^2 of 0.70 and RMSE of 28.5m^3 ha^{-1} when bands 1, 2, 3 and 4 of Quickbird satellite image were used as explanatory variables while Landsat 7 ETM+ satellite image gave R^2 of 0.54 and RMSE of 53.1 m^3 ha^{-1} with explanatory variables ETM2, 3 and 4.

Also Şenyurt et al. (2013) tried to derive multiple regression models for the stand parameters (volume, basal area and number of trees) using band brightness values obtained from Landsat 8 satellite image for Karşıkent state forest enterprise. For basal area, bands 2 and 4 were used as independent variables and gave coefficient of determination of 65.45% and 58.33% respectively. Likewise, mean stand diameters when regressed with band 2 as independent variable gave coefficient of determination of 49.25%.

Mısır (2013) carried out a study to estimate forest stand volume using Landsat 7 ETM+ and terrestrial measurements for the Trabzon KTÜ education and research forest. A total of 120 sample plots were used. Six bands' (1-5, 7) reflectance values and various vegetation indices were used as explanatory variables. The results of the regression models using 25 different vegetation index values as independent variables gave R^2 of 0.60, Syx of 36 m^3 and F of 25.

Çil (2015) investigated forest parameters such as the number of trees, basal area and volume to be obtained from field measurements via sample plots taken from the even aged

pure Scots pine (*Pinus sylvestris*) stands and uneven aged pure Fir (*Abies nordmanniana subs. bornmuelleriana*) stands. Kelkit/Gümüshane in which predominantly Scots pines are located and İğdir/Kastamonu regions which mainly consist of Fir stands were selected as the research areas. He used 5 different remote sensing data, including Göktürk-2, Rasat and aerial photographs taken by digital cameras previously unused for similar purposes to prove the relationship between stand parameters (the number of trees, basal area and volume) and the pixel values of the satellite images and different vegetation indexes. According to the obtained results, Landsat 8 satellite image gave highest estimates considering models developed for the estimation of number of trees, basal area and volume for both areas. Adjusted R square of volume and basal area models were found as 0.50 and 0.49 respectively in Kelkit and 0.48 and 0.43 for İğdir research area.

Günlü et al. (2015) tried to evaluate the compatibility of Landsat 7 ETM satellite image for predicting the dominant height in pure oriental beech stands in Göldag, Sinop. Firstly, the stand dominant height was determined by field measurements at total 70 sampling plots obtained from pure oriental beech stands. Then, reflectance values and vegetation indices were calculated based on the Landsat 7 ETM satellite data points that correspond to the sampling plots. The empirical relationships between stand dominant heights and the reflectance values and vegetation indices obtained from Landsat 7 ETM satellite image were derived using stepwise multiple regression analysis. The model dominant height using ETM 7 had an adjusted R^2 of 0.274. The other model dominant height using ND32 and ND54 had an adjusted R^2 of 0.390.

Çil et al. (2015) used 4 different remote sensing data, including Göktürk-2, Rasat, Landsat 8 satellite images and aerial photographs taken by digital camera to estimate volume, basal area and trees density for black pine stands (*Pinus nigra subs. pallasiana*) from Tetik (Kütahya) planning unit. In this study, satellite image pixel values (DN) and 160 samples obtained from areas with different vegetation indices (basal area, number of trees and stand volume parameters) indicated a relationship between them. According to the obtained results, Göktürk-2 satellite image gave highest estimates considering for number of trees 0,54 and Landsat 8 satellite imagine developed models with 0.59 and 0.67 adjusted R square respectively for volume and basal area.

Immitzer et al. (2016) used spectral and height information from the very high resolution WorldView-2 (WV2) satellite and angle-count sampling (ACS) national forest inventories (NFI) data for model training to generate wall to wall maps of growing stock for broadleaf, conifer and mixed forest stands using the non-parametric Random Forests (RF) algorithm as modeling approach.

It is observed that considerable number of researchers tried to use satellite imagery and inventory data to estimate some stand parameters. On the other hand, other remote sensing technologies can be utilized for the same purposes of estimating these vital forest parameters.

One of the recent remote sensing technologies in estimating forest stand volumes is LiDAR data. Light Detection and Ranging (LiDAR) is an established technology for obtaining accurate, high resolution measurements of surface elevations (Krabill et al., 1984). Airborne laser sensors allow scientists to analyze forests in a three-dimensional format over large areas. Unlike the traditional remote sensing methods, which yield information on horizontal forest pattern, modern LiDAR systems provide georeferenced information of the vertical structure of forest canopies. LIDAR data is being used to give a higher accuracy especially for forest height modelling.

However, despite use of LiDAR technology in forest management planning having been introduced and demonstrated on a small scale (Aydin, 2014), studies for Turkish forests are still missing except for a few papers done in Turkey but for study areas outside Turkey e.g. Akay et al. (2009) and Özdemir (2013). Therefore, for this Master thesis research, an area located in İzmir, Turkey was chosen to test the suitability of LiDAR data and WorldView-3 imagery for forest parameter estimation. The area was ideally suited for this purpose, as it was one of the few forest areas for which LIDAR data was readily available. This thesis thus looks at how best LiDAR data can be used to estimate some of the vital forest stand parameters and also when integrated with WorldView-3 imagery digital number (DN) values.

The overall objective of this research is to develop robust regression models to facilitate the use of LiDAR data in estimating plot volume (growing stock) and other forest parameters. The assumption taken was that field observed data was the accurate data. The specific objectives provide a general outline of the study approach and are as follows:

1. To develop robust processing and analysis techniques to facilitate the use of LiDAR data for predicting plot level tree heights and biomass/crown density.

2. To relate LiDAR-derived forest metrics to dominant plot height, mean plot height, stem number per hectare and volume per hectare.

3. To integrate LiDAR derived forest metrics and pixel values from Worldview-3 in estimating forest stand volume.

1.2. General Concepts

1.2.1. Brief Introduction and History of LiDAR

Currently, the most accurate method for collecting elevation data for the production of digital elevation or terrain models (DEMs or DTMs) is laser scanning or LiDAR (light detection and ranging or laser induced direction and ranging (Cavalli et al., 2008; Marks and Bates, 2000). The first laser instruments were built in the 1960s (Maiman, 1960; Smullins and Fiocco, 1962), with the first laser instrument for distance measurements invented in 1966 (Price and Uren, 1989). Non-scanning LiDAR systems were used for bathymetry, forestry and other applications in the 1970s and 1980s (Guenther, 2007; Nelson et al., 1984; Schreier et al., 1985; Solodukhin et al., 1977), which established the basic principles of using lasers for remote sensing purposes. The first experiments with modern laser scanner instruments were conducted in the early 1990s, and the first prototype of a commercial airborne laser scanning (ALS) system dedicated to topographic mapping was introduced in 1993.

LiDAR is an active remote sensing technology that determines ranges (i.e., distances) by taking the product of the speed of light and the time required for an emitted laser to travel to a target object. The elapsed time from when a laser is emitted from a sensor and intercepts an object can be measured using either (i) pulsed ranging, where the travel time of a laser pulse from a sensor to a target object is recorded; or (ii) continuous wave (CW) ranging, where the phase change in a transmitted sinusoidal signal produced by a continuously emitting laser is converted into travel time (Wehr and Lohr, 1999).

1.2.2. An Overview of LIDAR Systems

LiDAR systems are based on the principle of laser ranging. Young (1986) describes that with the laser process, a highly directional optical light can be created, thus yielding the high collimation and high optical power required for ranging. Lasers were demonstrated to be advantageous for this type of measurement as high-energy pulses can be realized in short intervals and short wavelength light can be highly collimated using small apertures. The laser, coupled with a receiver and a scanning system, enables the distribution and sensing of points over a swath defined by the instrument scan angle and flying height of the aircraft (Figure 1), whereas the distribution of points using earlier profiling systems were constrained to the along-track path of the aircraft.

LiDAR systems used in forestry applications can be categorized as either 'discrete return' systems or 'full waveform' systems and differ from one another with respect to how they vertically and horizontally sample a canopy's three-dimensional structure (Lim et al. 2003). Figure (2) shows this.

a = scan angle
h = flying height
s = swath width

$$s = 2 * h * \tan (a)$$

direction of flight
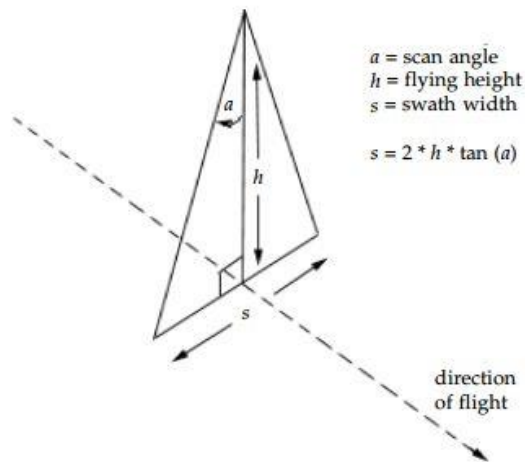
Figure 1. Swath width as a function of instrument scan angle and aircraft flying height

full waveform lidar

discrete return lidar
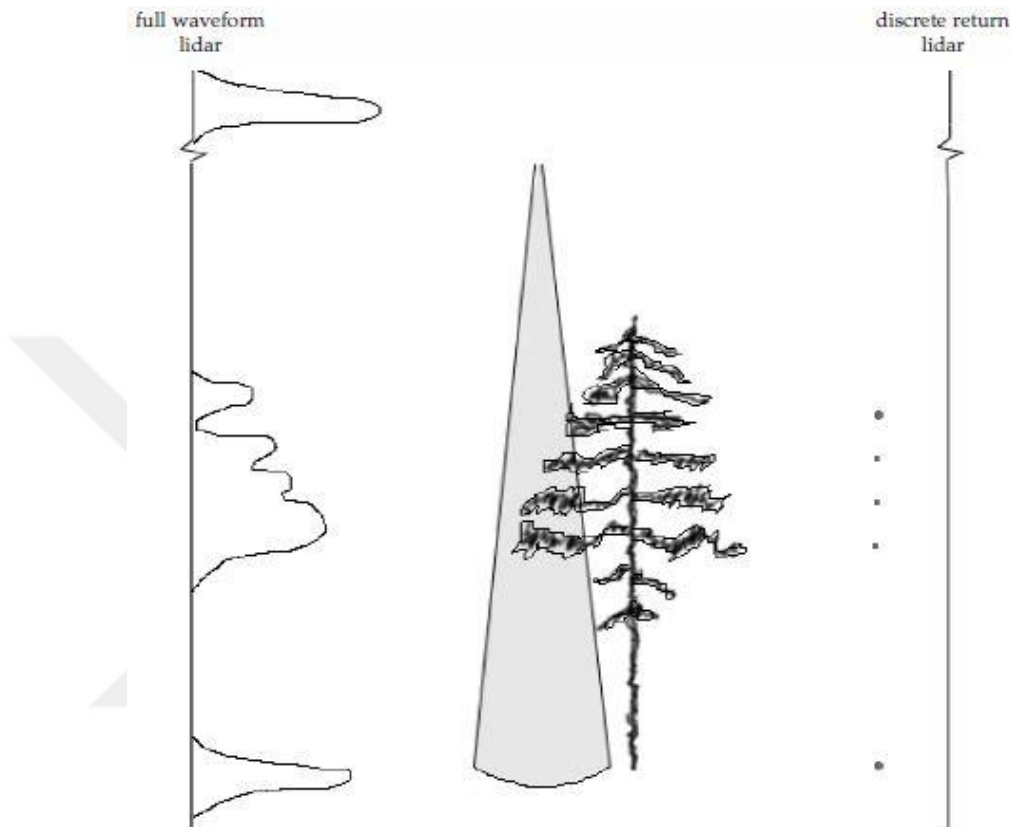
Figure 2. Differences between discrete return and full waveform vertical sampling

The vertical sampling of LiDAR systems relates to the number of range samples recorded for each emitted laser pulse. The horizontal sampling is determined by the area of the footprint and the number of such footprints, or 'hits', per unit area. Discrete return systems typically allow for one (e.g., first or last), two (e.g., first and last), or a few (e.g., five) returns to be recorded for each pulse during flight. Conversely, a full waveform LiDAR system senses and records the amount of energy returned to the sensor for a series of equal time intervals (Lim et al., 2003). The number of recording intervals determines the amount of detail that is present in a laser footprint. An amplitude-against-time waveform is constructed from each time interval and is representative of the area of interception. For forested

environments, the result is a waveform indicative of the forest structure (i.e., from the top of the canopy, through the crown volume and understory layer, and finally to the ground surface).

1.2.3. Brief History about LiDAR Remote Sensing of Forest Structure

Much of the original motivation for investigating the application of LiDAR in measuring forest attributes can be traced back to early studies by Arp et al. (1982), Nelson et al. (1984) and MacLean and Krabill (1986). MacLean and Martin (1984) used cross-sectional photogrammetric and densitometric methods to demonstrate that the cross-sectional area of a forest canopy profile was linearly related to the natural log of timber volume. It was assumed that if LiDAR could be used to develop accurate canopy profiles, then estimates of gross-merchantable volume could be made. Whereas earlier studies have been limited primarily by technology, more recent studies have benefited from a suite of scanning and profiling laser altimeters capable of recording a discrete quantity of laser returns or the full waveform of a pulse. The focus of earlier studies was on establishing statistical relationships between laser-derived measurements with ground-based measurements in the form of predictive linear models (Nelson et al., 1984). With significant advances in technology, the same needs exist to verify that new LiDAR systems are capable of matching previous results, if not improving upon them.

Various remote sensing systems and techniques have been explored for forestry applications as reviewed by a number of authors, e.g. Lefsky et al. (2001a) with a comparison of various remotely sensed data sources with LiDAR. Typically, most optical sensors are only capable of providing detailed information on the horizontal distribution and not the vertical distribution of vegetation in forests. LiDAR remote sensing is capable of providing both horizontal and vertical information with the horizontal and vertical sampling dependent on the type of LiDAR system used and its configuration (i.e., discrete return or full waveform LiDAR).

In the early 1980s, the Canadian Forestry Service demonstrated the applicability of profiling LiDAR for the estimation of stand heights, crown cover density and ground elevation below the forest canopy (Aldred and Bonner, 1985). In the same period, LiDAR was

utilized to map tropical forests in Central America (Arp et al., 1982). Krabill et al. (1980) showed that contouring data from LiDAR data and from photogrammetry techniques agreed within 12–27 cm in open areas and 50 cm in forested areas. Given the ability to accurately measure topography, it was realized that certain forest attributes could be quantified from forest canopy profiles derived from LiDAR data. Specifically, various forest attributes can be directly retrieved from LiDAR data, such as canopy height, subcanopy topography, and vertical distributions of canopies.

Besides volume and other related forest parameters, LiDAR data has also been used for other purposes in forestry. For example Shang et al. (2016) showed that due to the difficulties incurred to monitor/classify tropical forest areas when using remote sensing or in situ approaches because of their tremendous heterogeneity and complex structures, parameters directly derived from LiDAR measurements can be used to characterize the tropical forest biomes such as in distinguishing the rain and montane tropical forests from planted forests. Ellis et al. (2016) concluded that while ground based GPS is recommended as the most affordable method for wide-scale infrastructure mapping, aerial LiDAR is an effective tool for remotely quantifying the extent of logging impacts in tropical forests. Gonzalez et al. (2008) presented the accuracy evaluation of the LiDAR DTM data over forest planted field in order to use in forest harvest machinery assignment procedure, to finally delineate harvest units for spatial forest planning. JiLi et al. (2013) in their study titled "classification of tree species on structural features derived from high density LiDAR data" demonstrated the significance of the LiDAR derived structural features as aids to classify tree species and their results showed a positive linear correlation (R^2=0.88) between LiDAR point density and species classification accuracy.

Recent studies have also shown attributes that can be predicted using empirical models from LiDAR data such as above-ground biomass, basal area, mean stem diameter, vertical foliar profiles and canopy volume (Means et al., 1999; Lefsky et al., 1999a; Lefsky et al., 1999b; Dubayah and Drake, 2000).

Akay et al. (2009) indicated that LiDAR based forest structure data and high-resolution digital elevation models (DEMs) can be used in wide-scale forestry activities such as stand characterizations, forest inventory and management, fire behavior modeling, and

forest operations. More and more studies have been done recently in modelling forest parameters using LiDAR data world over.

Most of the research about LiDAR in forestry follow a proposed practical two-stage procedure for prediction of corresponding characteristics of forest stands that was developed and tested by (Nasset, 2002). In this study his proposed practical two-stage procedure was tested on sixty-one stands with an average size of 1.6 ha each and divided into 200 m^2 regular grid cells. The six examined characteristics were predicted for each grid cell from the corresponding laser data utilizing the estimated regression equations. Average values for each stand was computed. Most stand level predictions were unbiased (P > 0.05). Standard deviations of the differences between predicted and ground-truth values of mean height, dominant height, mean diameter, stem number, basal area, and volume were 0.61–1.17 m, 0.70–1.33 m, 1.37–1.61 cm, 16.9–22.2% (128–400 ha^{-1}), 8.6–11.7% (2.33–2.54 m^2 ha^{-1}), and 11.4–14.2% (18.3–31.9 m^3 ha^{-1}), respectively. In another study Nasset et al. (2001), the mean heights of dominant trees and the stem numbers of 39 plots of 200 m^2 each were derived from various canopy height metrics and canopy density measured by means of a small-footprint airborne laser scanner over young forest stands with tree heights < 6 m. Ground-truth values were regressed against laser-derived canopy height metrics and density. The regressions explained 83% and 42% of the variability in ground-truth mean height and stem number, respectively. Cross validation of the regressions revealed standard deviations of the differences between predicted and ground-truth values of mean height and stem number of 0.57 m (15%) and 1209 ha^{-1} (28.8%), respectively.

Chen et al. (2012) carried out a study titled 'A GEOBIA framework to estimate forest parameters from LiDAR transects, Quickbird imagery and machine learning: A case study in Quebec, Canada'. Forest parameter estimation results derived from their GEOBIA framework demonstrate a strong relationship with those using the full LiDAR cover; where the highest estimates for canopy height (R = 0.85; RMSE = 3.37 m), AGB (R = 0.85; RMSE = 39.48 Mg/ha) and volume (R = 0.85; RMSE = 52.59 m^3/ha) were achieved using a LiDAR transect sample representing only 7.6% of the total study area.

González-Ferreiro et al (2012) tried to estimate stand variables in *Pinus radiata* plantations using different LiDAR pulse densities. The models tested use LiDAR-derived

canopy height and intensity distribution metrics as explanatory variables to predict the following stand attributes: mean height, dominant height, stand basal area, stand volume, stand crown biomass, stand stem biomass and stand aboveground biomass. Exponential models performed best in most cases, with goodness-of-fit statistics similar to those reported in the international literature for boreal forests. The coefficient of determination ranged from 0.44 (for stand crown biomass) to 0.87 (for dominant height), and the root mean square error/mean·100 ranged from 8.2 per cent (for dominant height) to 31.6 per cent (for stand stem biomass). Model precision did not essentially vary after reducing 94 per cent of the original point cloud, i.e. when laser pulse density was reduced from 8 pulses m^{-2} to only 0.5 pulses m^{-2}.

Shataee (2013) in his study titled 'forest attributes estimation using aerial laser scanner and TM data' aimed at analyzing performance of four non-parametric algorithms including the k-NN, SVR, RF and ANN to estimate forest volume and basal area attributes using combination of Aerial Laser Scanner and Landsat TM data. Results showed that among four methods, SVR using the RBF kernel could better estimate volume/ha with lower RMSe and bias (156.02 m^3 ha^{-1} and 0.48, respectively) compared to others. In basal area/ha, k-NN could generate results with similar RMSe (11.79 m^3 ha^{-1}) but unbiased (0.03) compared to SVR with RMSe of 11.55 m^3 ha^{-1} but slightly biased (–1.04).

Mora et al. (2013) in their study tried to model stand height, volume, and biomass from very high spatial resolution satellite imagery and samples of airborne LiDAR. Stand and tree objects were delineated, followed by modeling of stand height, volume, and AGB using metrics derived from the stand and tree crown objects. The calibration and validation of the models were based on co-located LiDAR derived estimates. A k-nearest neighbor approach provided the best accuracy for stand height estimation ($R^2 = 0.76$, RMSE = 1.95 m). Linear regression models were the most efficient for estimating stand volume ($R^2 = 0.94$, RMSE = 9.6 m^3 ha^{-1}) and AGB ($R^2 = 0.92$, RMSE = 22.2 t ha^{-1}). This study was implemented for one Canadian ecozone and demonstrated the capacity of a methodology to produce forest inventory attributes with acceptable accuracies offering potential to be applied to other boreal regions.

Unger et al. (2014) assessed the utility of using LiDAR data to estimate number of trees, tree height and crown width within Barksdale Air Force Base forest management area, Bossier City, Louisiana. Two programs, LiDAR Data Filtering and Forest Studies (Tiffs) and Lidar Analyst were used to derive forest measurements, which were compared to field measurements. Based on Root Mean Square Error (RMSE), Lidar Analyst (3.81 trees) performed better than Tiffs (5.71 trees) at estimating average tree count per plot. Tiffs was better at deriving average tree height than Lidar Analyst with an RMSE of 19.08 feet to Lidar Analyst's RMSE of 21.20 feet. Lidar Analyst, with a RMSE of 25.41 feet, was better in deriving average crown diameter over Tiffs RMSE of 30.54 feet. All linear correlation coefficients between average field measured tree height and Lidar derived average tree height were highly significant at the 0.01 probability level for both Tiffs and Lidar Analyst on hardwood, conifers and a combined hardwood conifer comparison.

Kwak et al. (2014) used almost similar procedure to estimate plot volume using LiDAR height and intensity distributional metrics. The candidate variables for predicting plot volume were evaluated using three data sets: total, canopy, and integrated LiDAR height and intensity metrics. The use of three data sets was statistically significant at $R^2 = 0.75$ (RMSE = 52.17 m^3 ha^{-1}), $R^2 = 0.84$ (RMSE = 45.24 m^3 ha^{-1}), and $R^2 = 0.91$ (RMSE = 31.48 m^3 ha^{-1}) for total, canopy, and integrated LiDAR distributional metrics, respectively.

Azita et al. (2015) presented an approach for estimating tree heights, stand density and crown patches using LiDAR data in a subtropical broad-leaved forest. The study was conducted within the Yambaru subtropical evergreen broad-leaved forest, Okinawa main island, Japan. A digital canopy height model (CHM) was extracted from the LiDAR data for tree height estimation and a watershed segmentation method was applied for the individual crown delineation. Dominant tree canopy layers were estimated using multi-scale filtering and local maxima detection. The LiDAR estimation results were then compared to the ground inventory data and a high resolution orthophoto image for accuracy assessment. A Wilcoxon matched pair test suggests that LiDAR data is highly capable of estimating tree height in a subtropical forest (z = 4.0, p = 0.345), but has limitation to detect small understory trees and a single tree delineation. The results show that there is a statistically significant different type of crown detection from LiDAR data over forest inventory (z = 0, p = 0.043). They also found

that LiDAR computation results underestimated the stand density and overestimated the crown size.

Also Maack et al. (2016) in their study titled "Modelling the standing timber volume of Baden-Württemberg—A large-scale approach using a fusion of Landsat, airborne LiDAR and National Forest Inventory data" used a unique wall-to-wall air-borne LiDAR dataset and Landsat 7 satellite images in combination with terrestrial inventory data derived from the National Forest Inventory (NFI), and applied generalized additive models (GAM) to estimate spatially explicit timber distribution and volume in forested areas. Furthermore, they balanced the training dataset with a bootstrap method to achieve unbiased regression weights for interpolating timber volume. The model performance of the original approach was ($r^2 = 0.56$, NRMSE = 9.65%), the approach with balanced training data ($r^2 = 0.69$, NRMSE = 12.43%) and the final approach with balanced training data and the additional socio-economic predictor ($r^2 = 0.72$, NRMSE = 12.17%).

Giannico et al. (2016) in their study assessed forest stand volume and above-ground biomass (AGB) in a broadleaved urban forest, using a combination of LiDAR-derived metrics, which takes the form of a forest allometric model. They tested various methods for extracting proxies of basal area (BA) and mean stand height (H) from the LiDAR point-cloud distribution and evaluated the performance of different models in estimating forest stand volume and AGB. The best predictors for both models were the scale parameters of the Weibull distribution of all returns (except the first) (proxy of BA) and the 95th percentile of the distribution of all first returns (proxy of H). The R^2 were 0.81 ($p < 0.01$) for the stand volume model and 0.77 ($p < 0.01$) for the AGB model with a RMSE of 23.66 $m^3 ha^{-1}$ (23.3%) and 19.59 $Mg.ha^{-1}$ (23.9%) respectively.

1.2.4. LiDAR Technology in Turkey's Forestry Sector

Akay et al. (2009) conducted a study to investigate the capabilities and advantages of using LiDAR remote sensing technology in various forestry applications based on previously conducted studies. Their results indicated that LiDAR based forest structure data and high-resolution DEMs can be used in wide-scale forestry activities such as stand characterizations, forest inventory and management, fire behavior modeling, and forest operations. Özdemir

(2013) carried out a study titled "Estimation of forest stand parameters using airborne LIDAR data" for an area near Newcastle city in England. His findings were that if stands parameters are estimate with LiDAR data in complex forest ecosystems, the forest stands should be pre-stratified by definite criteria. The regression models developed by means of stepwise selection procedure explained 0.82% and 0.70% of the variation in number of trees and mean diameter at breast height respectively and concluded that number of trees and mean diameter at breast height can be predicted at plot level in conifer dominated forest stands using airborne laser scanning data (Aydin, 2014).

Also worth mentioning is that the forest management planning department under General Directorate of Forestry decided to integrate LiDAR technology in forest management planning after a variety of meetings in 2014 as reported by Aydin in the report. High profile individuals from the General Directorate of Forestry had series of meetings on how LiDAR technology can be of use in the preparation of forest management plans like has been the case in other countries like Finland, Austria, etc. Experts from Austria, which is advanced in use of LiDAR in forestry, were also part of these meetings. With these meetings LiDAR technology use in forestry was introduced in Turkey. In September 8-11, 2014, an education software of how LiDAR works in forestry was developed. Las LiDAR point cloud data was used and digital terrain model (DTM) as well as digital surface model (DSM) were produced. All other necessary processes were performed and with non-forest areas masked out from the study area leaving only forested areas. The following results were obtained for each forestry polygon;

- Average height
- Average slope
- Dominant height
- Average stand height
- Number of trees per hectare
- Crown Closure
- Canopy space integral (CSI)
- Stand Volume
- Forest Road Network

However, the generalization of LIDAR technology to countrywide was not suggested on the basis of some reservations such as absence of the field survey to test the results, high operation costs, limitations of directly getting tree species, development stage and crown cover, hard to use for broadleaved species, requirements for additional software and trained staff, difficulties in obtaining other parameters like quality or removable trees (Aydin, 2014).

1.2.5. Worldview Imagery in Forestry

The identification of species within an ecosystem plays a key role in formulating an inventory for use in the development of forest management plans. Plant species mapping with remote sensing is linked to an understanding that species have unique spectral signatures associated with characteristic biochemical and biophysical properties (Asner and Martin, 2009; Clark et al., 2005). However, widespread mapping of species at the regional scale has been hampered by the low spectral resolution of most existing space borne sensors (e.g. Landsat, Systeme Probatoire d'Observation de la Terre (SPOT) and Quickbird) and the scarcity of appropriate high spectral resolution (hyper spectral) sensors (Huang and Asner, 2009). This low spectral resolution in most existing space borne sensors can be improved with integration of LiDAR data. Apostol et al. (2010) concluded that high density points LiDAR data combined with high resolution imagery are the best choice for improved results in precision forestry. Zald et al. (2016) integrated Landsat pixel composites and change metrics with LiDAR plots to predictively map forest structure and aboveground biomass in Saskatchewan, Canada. Their imputation model had moderate to high plot-level accuracy across all forest attributes (R^2 values of 0.42-0.69), as well as reasonable attribute predictions and error estimates (for example, canopy cover above 2 m on validation plots averaged 35.77%, with an RMSE of 13.45%. Their study demonstrated that using LİDAR plots and pixel compositing in imputation mapping can provide forest inventory and monitoring information for regions lacking ongoing or up-to-date field data collection programs.

In 2009, WorldView-2was launched by DigitalGlobe. The very high spatial resolution (0.5 m in the panchromatic band and 2.0 m in the multispectral bands) and 4 new spectral bands (Coastal, Yellow, Red Edge and Near Infrared 2) additional to the 4 standard bands (Blue, Green, Red, and Near Infrared 1), give reason to expect that this sensor has a high

potential for tree species mapping. All 4 new bands are strongly related to vegetation properties. For example, the reflectance measured in the Coastal band is related to the chlorophyll content of plants. The Yellow band is intended for the detection of 'yellowness' of targets, for example, of tree crowns caused by insect diseases. The Red Edge band is supposed to discriminate between healthy trees and trees that are impacted by disease and to enhance the separation between different species and age classes. The Near Infrared 2 band that partly overlaps the standard Near Infrared 1 band but is less affected by atmospheric influence is expected to enable sophisticated vegetation analysis, such as biomass studies (URL-2, 2016).

Not many studies have been done in which worldview imagery is integrated with LiDAR data especially for purposes of forest structure prediction. Qiu and Zhou (2015) fused high spatial resolution WorldView-2 imagery and LiDAR pseudo-waveform for object-based image analysis and the fused dataset achieved an overall classification accuracy of 97.58%, a Kappa coefficient of 0.97 and producer's accuracies and user's accuracies all larger than 90%. Straub et al. (2013) assessed the use of Cartosat-1 and WorldView-2 stereo imagery in combination with LiDAR-DTM for timber volume estimation in a highly structured forest in Germany. At plot level the following root mean squared errors (RMSEs) for timber volume estimation were obtained: 50.26 per cent for Cartosat-1, 44.40 percent for WorldView-2 and 38.02 per cent for LiDAR. The RMSEs were smaller than the standard deviation of the observed timber volume. The RMSEs at a stand level yielded 21.49 per cent for Cartosat-1, 19.59 per cent for WorldView-2 and 17.14 per cent for LiDAR.

WorldView-3 was launched on August 13, 2014 by Digital Globe. Besides offering 30 cm resolution panchromatic and eight-band visible and near-infrared (VNIR) imagery, WorldView-3 collects shortwave infrared (SWIR) imagery in eight-bands. This allows the satellite to sense the VNIR spectrum as well as expand deeper into the infrared spectrum than any other commercial imaging satellite, providing rich data for precisely identifying and characterizing manmade and natural materials. WorldView-3's eight SWIR bands span the spectrum's three atmospheric transmittance imaging windows to capture unique information for materials identification, wildfire response, food security, mining/geology, and other applications. WorldView-3 is the first commercial satellite to have 16 high-resolution spectral

bands that capture information in the visible and near-infrared (VNIR) and short-wave infrared (SWIR) regions of the electromagnetic spectrum (EMS). Operating at an altitude of 617 kilometers, the satellite provides 31 cm panchromatic resolution, 1.24 m VNIR resolution, and 3.7/7.5 m SWIR resolution, according to their operating licenses (Department of Commerce). WorldView-3 builds upon WorldView-2's unique capabilities, providing eight additional spectral bands farther into the SWIR portion of the EMS. This spectral expansion enhances WorldView-3's capability to capture the uniqueness of each ground material's spectral signature. Due to minimal atmospheric influence or noise in this part of the EMS, as well as an enhanced ability to differentiate among ground materials, the SWIR bands open the door for automated information extraction to save time, money and possibly lives.

WorldView-3's 16 spectral bands allow for automated information extraction for various applications. Because WorldView-3 provides continuity of WorldView-2 VNIR bands at a higher spatial resolution as well as a revolutionary sensor with eight new SWIR spectral bands offered on a commercial satellite for the first time, the satellite is helping to transform the remote sensing industry from a pixel-based industry into a product-based industry, expanding the use of remotely sensed data to create ways to better understand and manage our changing planet (URL-2, 2016). In forestry applications, one of the amazing things that SWIR enables is the ability to see through the dense smoke of an active fire to the ground beneath, as well as locating the flame front and hot spots in the fire (URL-3, 2016).

However no studies were found in which WorldView-3 imagery has been used together with LiDAR data for purposes of estimating forest structures. With the results of the various studies outlined above that used WorldView-2 imagery and LiDAR data, it is highly expected that with this new high resolution imagery better results can be obtained for both classification of forests and estimation of forest structures.

.

2. Methodology

2.1. Study Area

The study area of this research is part of Yenisakran Forest Management unit of Bergama State Forest Enterprise which is under the jurisdiction of Izmir Regional Directorate of Forestry. The study area was chosen because it is part of the area on which airborne laser scanning (ALS) in form of LiDAR data was recently conducted by Turkey's General Command of Mapping.
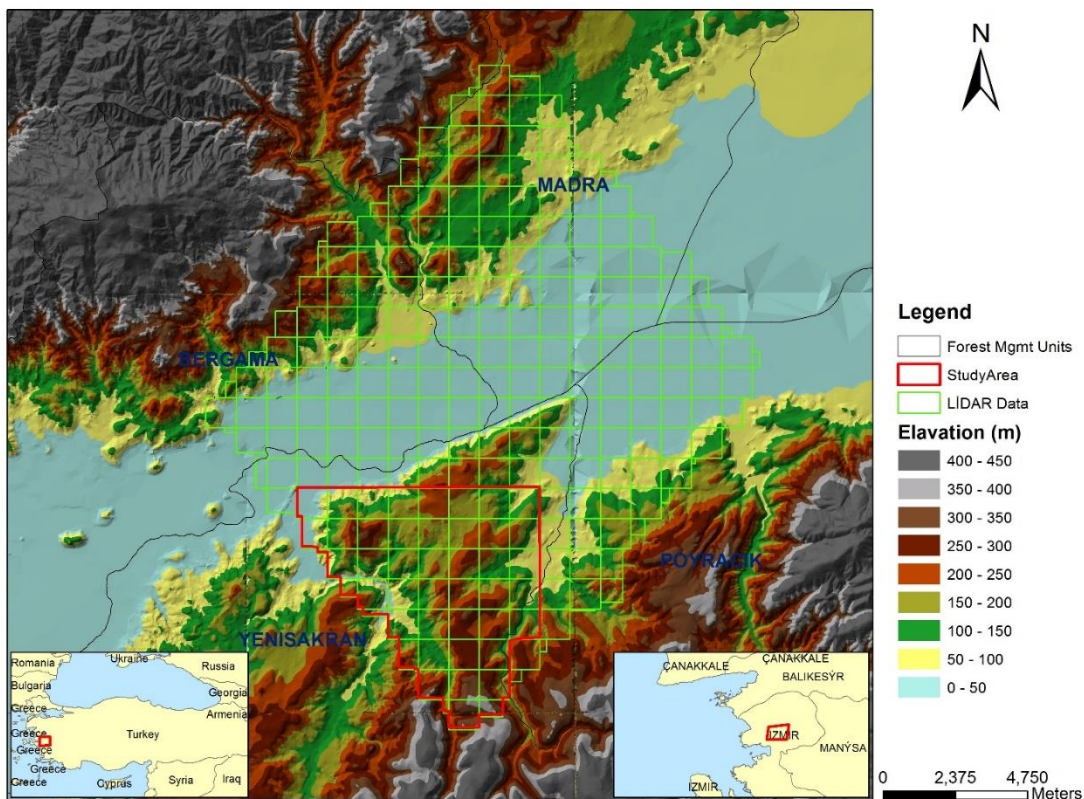
Figure 3. Spatial location of the study area

The area is located in the northern part of Izmir, Turkey in a township called Bergama. It has an area of approximately 7000 ha (Figure 3). The study area is composed mainly of

Turkish Red pine *(Pinus brutia Ten.)* referred to as Kızılçam in Turkish. Most of the land is used for agricultural purposes with a few mining areas and human settlements while the rest are forest stands ranging from young, medium and mature stands as well as degraded forest stands. Figure 4 shows land use map based on the forest management plan of 2008. The stand boundaries of all stands in the study area were obtained from the Forest Directorate as coordinated GIS shape files with projected coordinate system ED_1950_UTM_Zone_35N (GDF, 2008). The stands were re-classified according to criteria such as land use, age class and development stage for sampling purposes.
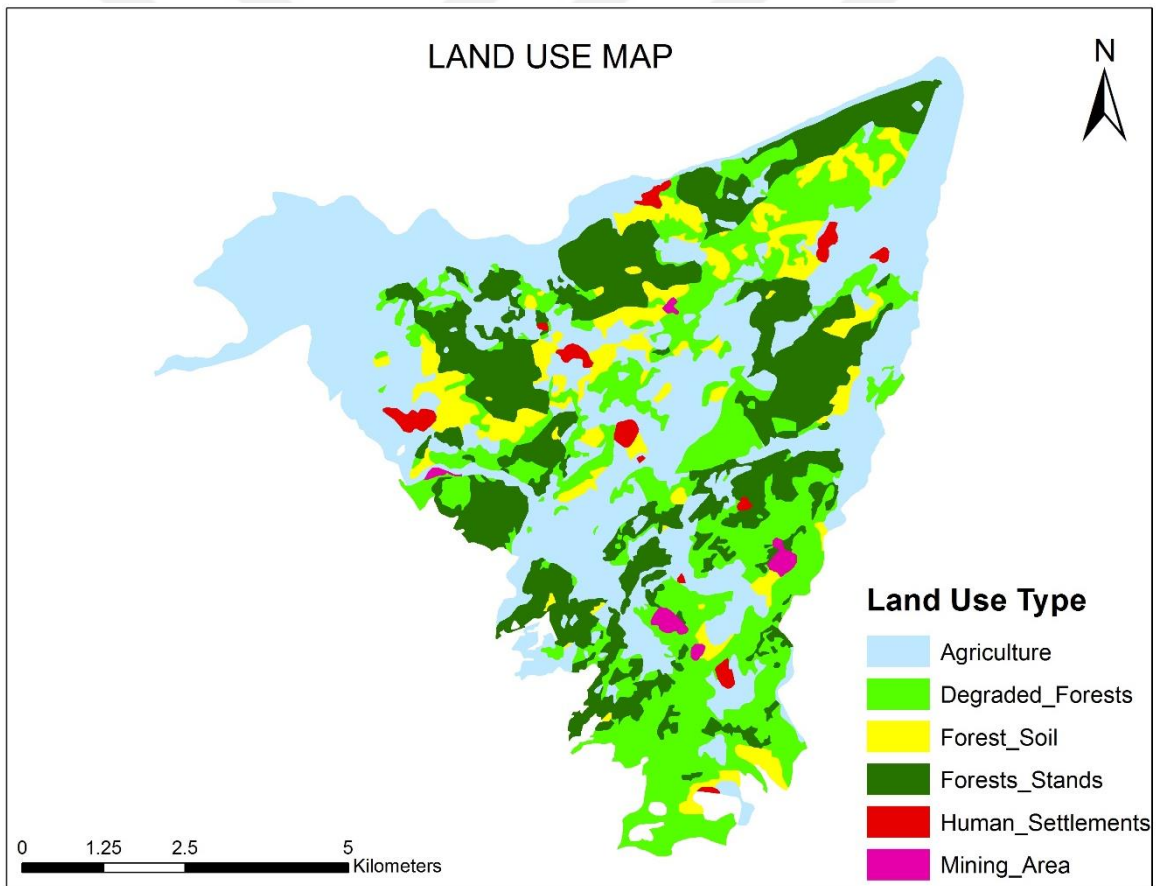
Figure 4. Study Area land use map

A total of 58 points were randomly created in ArcGIS with minimum spacing of 300 m with a condition that each stand type is well represented and a buffer was made around

each of these random points thereby making each sampled point a sample plot (Figure 5). The study area comprised of a total of 16 stand types of pure Turkish Red pine representing various combinations of age classes.

In order not to confuse the forested areas from non-forested areas during sample plot creation, a forest mask was established based on the shape file maps obtained as part of the forest management plan for the study area.
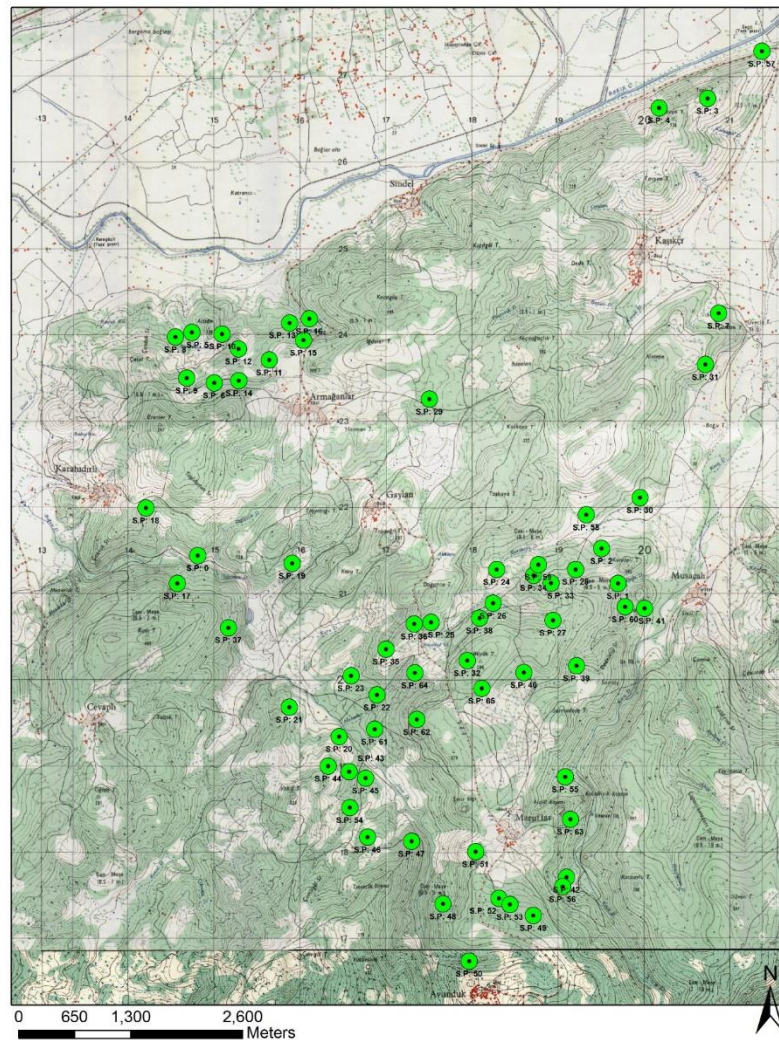
Figure 5. Sample points

2.2. Sample Plot Field Inventory

During field data collection, the center of each plot was located using GPSMAP 64s global positioning system (GPS). The actual x, y coordinates for each sample plot were recorded and later were spatially registered and stored in a GIS. These were the sample point coordinates on which buffers were made. Data collection was done between April 24th and May 1st 2016. The sizes of sample plots (area) were made in accordance with the standard inventory design of the functional planning approach instructions as applied in Turkey in which case the crown cover is used as basis to come up with a reasonable sample area that would give a fair representation of forest characteristics for that particular forest area. With this rule; 12 sample plots had an area of 200m^2 each, 18 sample plots had an area of 400m^2 each, 12 sample plots had an area of 600m^2 each and 16 sample plots had an area of 800m^2 each. In the field, the following forest parameters were measured; the diameter at breast height of each tree (dbh) >= 8, age of one of the dominant trees, height of at least a couple of trees to represent the dominant plot height and also the co-dominant plot height. Other parameters of importance to this study observed were the crown cover of the shrubs in percentage as well as their average heights.

The heights were measured using the Haglof Vertex IV ultrasound instrument system. Average height was based on measured tree heights of trees with dbh > 8 cm, which conforms to ordinary inventory practice. Dominant height of each plot was computed as the arithmetic mean height of the 100 largest trees per hectare according to diameter, which is a commonly used definition (Tveite, 1977). Volume of trees per sample plot was calculated using the yield models for Turkish red pine (GDF, 2008) that takes into account only the diameter designed for Yenişakran planning unit. For each sample, each tree with a dbh of 8 cm and above was measured and volume calculated and later the total volume of all trees in that sample represented the total tree volume. Since LiDAR data was acquired in October 2014 and field inventory in April 2016, an adjustment of one growing season was done on calculated field measured volume using the yield tables so as to harmonise the two different data collection periods. Out of the 58 random sample points made in ArcGIS, only 43 sample points were

visited. This was because some random points were falling on road ways, agricultural field plantations etc. while others were simply inaccessible. Table 1 shows the field data collected.

Figure 6. Field inventory data collectors; Bayram, Uzay (supervisor) and Kennedy

Table 1. Some parameters obtained from field survey

S.P No	Area m^2	No. of Trees	Trees per ha	Dominant Height (m)	Av. Height m	Total Volume (m^3)	Volume per Ha	Shrub C.C %	Shrub Height (m)
2	600	19	317	10.8	8.7	2.215	36.9	10	1.7
6	400	17	425	15.7	13.3	4.158	103.9	30	1
7	400	32	800	15.2	13.4	8.377	209.4	35	1.5
9	800	20	250	21.6	13.8	7.194	89.9	80	2
10	400	13	325	20.2	17.3	10.207	255.1	25	1.6-1.7
11	400	18	450	24.6	20.	10.077	251.9	40	1.3-1.4
13	800	6	75	14.4	9.92	1.531	19.1	10	3.5-4
16	600	12	200	15.4	12.7	5.509	91.8	100	3.5-4
21	800	8	100	31.1	25	12.888	161.1	5	0.7-0.8
23	600	13	217	20.1	16.1	13.15	219.1	0	0
24	600	10	167	20.2	15.4	16.872	281.2	65	1.6-1.7
25	800	26	325	28.5	21.5	10.193	127.4	40	1.7
26	800	14	175	18.4	15.3	8.803	110.0	10	1.3-1.4
27	400	14	350	16.1	12.2	6.621	165.5	30	1.5
28	400	31	775	15.2	11.9	5.965	149.1	35	1.5-1.6
29	400	40	1000	11.1	8.9	3.301	82.5	10	3
30	400	27	675	15.2	12.3	7.878	196.9	80	2.5-3
31	400	17	425	16.4	14.6	6.047	151.2	15	1
32	400	18	450	14.9	12	3.952	98.8	90	4-4.5
33	600	35	583	14.6	8.5	5.405	90.1	10	1.3
35	600	12	200	27.9	23.6	11.626	193.7	5	1.8-1.9
36	800	13	163	24	21.5	15.675	195.9	30	2.5-3
37	600	18	300	19.5	14.3	10.147	169.1	40	1.7
39	400	19	475	15.8	14.5	3.858	96.4	10	4-4.5
40	600	9	150	14	11.3	2.347	39.1	100	3.5-4
41	800	9	113	8.9	6.8	0.809	10.1	60	3-3.2
42	600	8	133	17.3	15.4	6.571	109.5	20	2-2.5
43	400	22	550	11.3	10.9	6.700	167.5	85	1.9
45	800	6	75	11.8	10.1	2.016	25.2	50	3-3.5
46	400	20	500	19.2	16.4	5.449	136.2	0	0
50	800	18	225	12	11.1	5.247	65.5	90	2.1
52	800	12	150	8.7	6.4	2.200	27.5	80	1.6-1.7
53	800	15	188	10.3	7.9	4.717	58.9	40	2.1
54	600	23	383	10.4	8.5	5.937	98.9	60	2
55	400	27	675	18.7	17.1	10.403	260.1	5	1.6-1.7
57	400	17	425	14.6	10.9	8.122	203.1	65	1.7
59	600	17	283	19	16.3	8.426	140.4	25	2.5-3.0
60	400	22	550	22.8	18.2	8.829	220.7	0	0
61	800	7	88	12	10.9	3.383	42.3	35	2.5
62	200	35	1750	16.2	12.5	1.904	95.2	4	0.5-0.6
63	600	12	200	20.2	16	12.598	209.9	80	3-3.5
65	800	12	150	20.8	13.6	7.212	90.1	0	0
66	800	14	175	14.4	11.65	6.179	77.23	80	3.5-4

2.3. LiDAR Data

2.3.1. General Information and LiDAR Data Pre Processing

The LiDAR data used in this study was acquired on 21st and 22nd of October 2014 using an LMS-Q1560 LiDAR system of Riegl Inc. belonging to the Turkish General Command of Mapping that was mounted on a Beechcraft-200 aircraft (Kayı et al., 2015). The specifications of this LiDAR system are shown in (Table 2).

Table 2. Riegl LMS-Q1560 Technical Specifications

Flight Altitude	400-4700 m
Effective Laser Frequency	200-800 kHz
Scanning Angle	$58/60^{o}$
Accuracy	2 cm (250m)
Scanning Mechanism	Rotative

Main properties of the acquired LiDAR datasets were; altitude of 1200 m, sampling density $<= 8$ points m^{-2}, scanning angle of 30° and at a speed of 150 knots (approximately 77.2 m s^{-1}). Twenty nine flight lines with approximately 50% overlap were flown (Kayı et al., 2015).

The area flown covers parts of four forest management units of Bergama State Enterprise namely; Bergama, Yenisakran, Madra, and Poyracik as shown in figure (3). The ready LiDAR data in form of classified las files was obtained from the General Command of mapping headquarters in Ankara, Turkey. It must be pointed out that this LiDAR data is part of the LiDAR test flight done by the General Command of Mapping, among the first of its kind in Turkey. The General Command of Mapping also pointed out that for this specific LiDAR system (Riegl), the ground control was not used to check the system in detail and that this was to be done at a later stage (Kayı et al., 2015). Due to the above reason and also the fact that the LiDAR test flight was not done for the sole purpose of use in forestry, the data had to be filtered and some points reclassified as noise points so that they do not interfere in

the production of models. The classification and reclassification was done using lastools (Figure 7).

Also worth noting is that LiDAR data used in this study is above recommended scanning angle of 0-10°. Scanning angle is said to have an effect on mean height and volume estimations (Leckie 1990; Nasset 1997a) and this is why LiDAR data with a scanning angle between 0 and 10 degrees have small errors when estimating small heights (Magnussen and Boudewyn 1998).

Noise points were removed in lastools. The condition for a point to be classified as noise was using 1m in xy direction and 0.2 m in z direction and 3 points as being isolated as shown in Figure 8. After removing noise purported points, the average point density for both ground points and non-ground points were reduced to 1-3 points m^{-2}. Parker and Glass (2004) and Smreček and Danihelová (2013) defined low-density LiDAR data to have densities of 1 point m^{-2} or less. However, Smreček and Danihelová (2013) classified high point density to be above 10 points m^2, whereas Parker and Glass (2004) defined high point density to be above 4 points m^{-2}. Therefore, the LiDAR points used in this study were classified as low-density data in accordance with the definitions of previous studies.
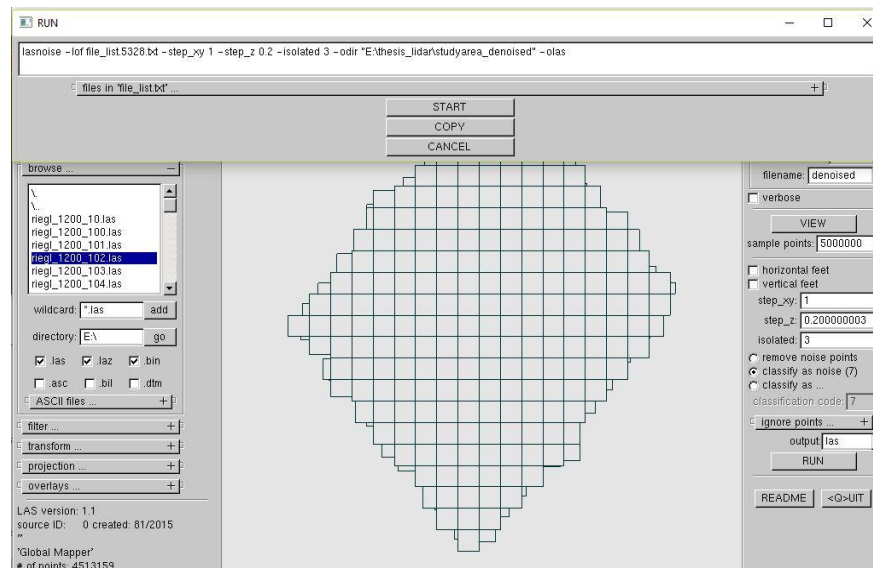
Figure 7. Screen print of las tools-noise point classification

2.3.2. LiDAR Derived Models

Ground and vegetation cloud points, after classification and reclassification, were used to produce a Digital Terrain Model (DTM) and a Digital Surface Model (DSM) respectively with a geometric resolution of 1 m using ArcGIS and TreesVis software (an algorithm developed by the Professorship of Remote sensing and Landscape Information Systems (FELIS) of the Faculty of Environmental and Natural Resources, University of Freiburg, Germany). The Canopy Height Model (CHM) was then calculated as result of the algebraic subtraction of DTM from DSM using the Minus tool found in the ArcGIS 10.2 ^{TM} Spatial Analyst toolbox (ArcToolbox\Spatial Analyst Tools\Math\Minus). The CHM gives the height of upper canopy for each any pixel included in the surveyed forest. The few negative values of less than one meter are a result of differing processing methods of DTM and DSM in ArcGIS while the high values of as much as 84.4 m are as a result of other objects in air such as birds flying and so on. Figures 8, 9 and 10 show the produced DTM, DSM and CHM.

To calculate biomass or canopy density, bare earth multipoint and aboveground multipoint feature classes were made in ArcGIS (ArcToolbox\3D Analyst Tools\Conversion\From File\LAS to Multipoint). The multipoint feature classes where then converted to raster files. This was done with the Point to Raster tool in ArcGIS (ArcToolbox\Conversion Tools\To Raster\Point to Raster). When calculating density, the number of returns in a given area is important rather than the elevation values returned, so the value field on the Point to Raster form is irrelevant (Esri, 2011). As end result, the canopy returns are divided by the total returns to get the canopy density also referred to as canopy return ratio. Dense canopy is represented by a value of 1.0, and no canopy is represented by a value of 0. Figure 11 shows the produced canopy density. Canopy return ratio is calculated as shown in equation 1.

$$\text{Canopy Density (Canopy Return ratio)} = \frac{The\ number\ of\ Canopy\ returns}{The\ number\ of\ total\ Returns} \qquad \text{Eq. 1}$$
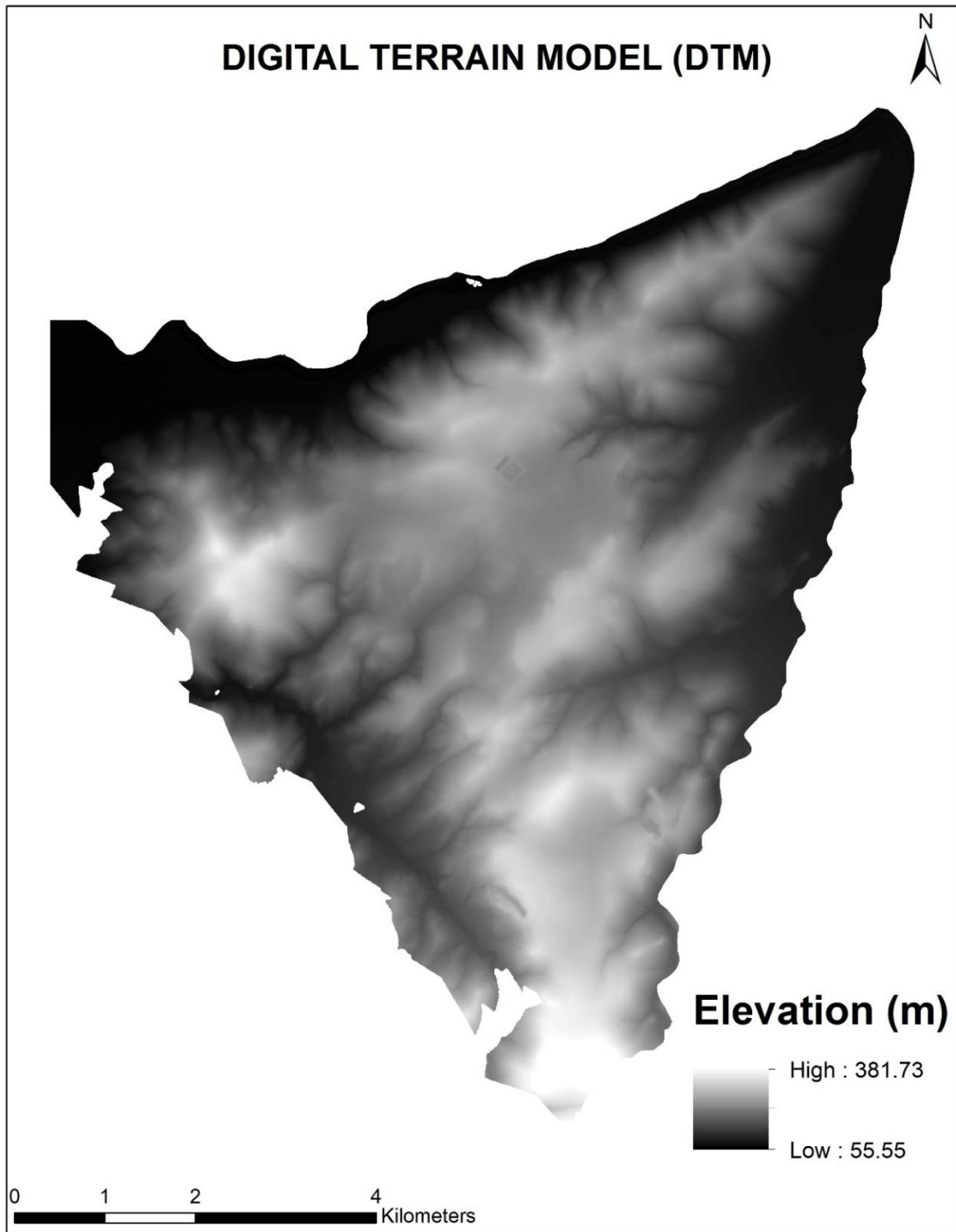
Figure 8. Digital Terrain Model
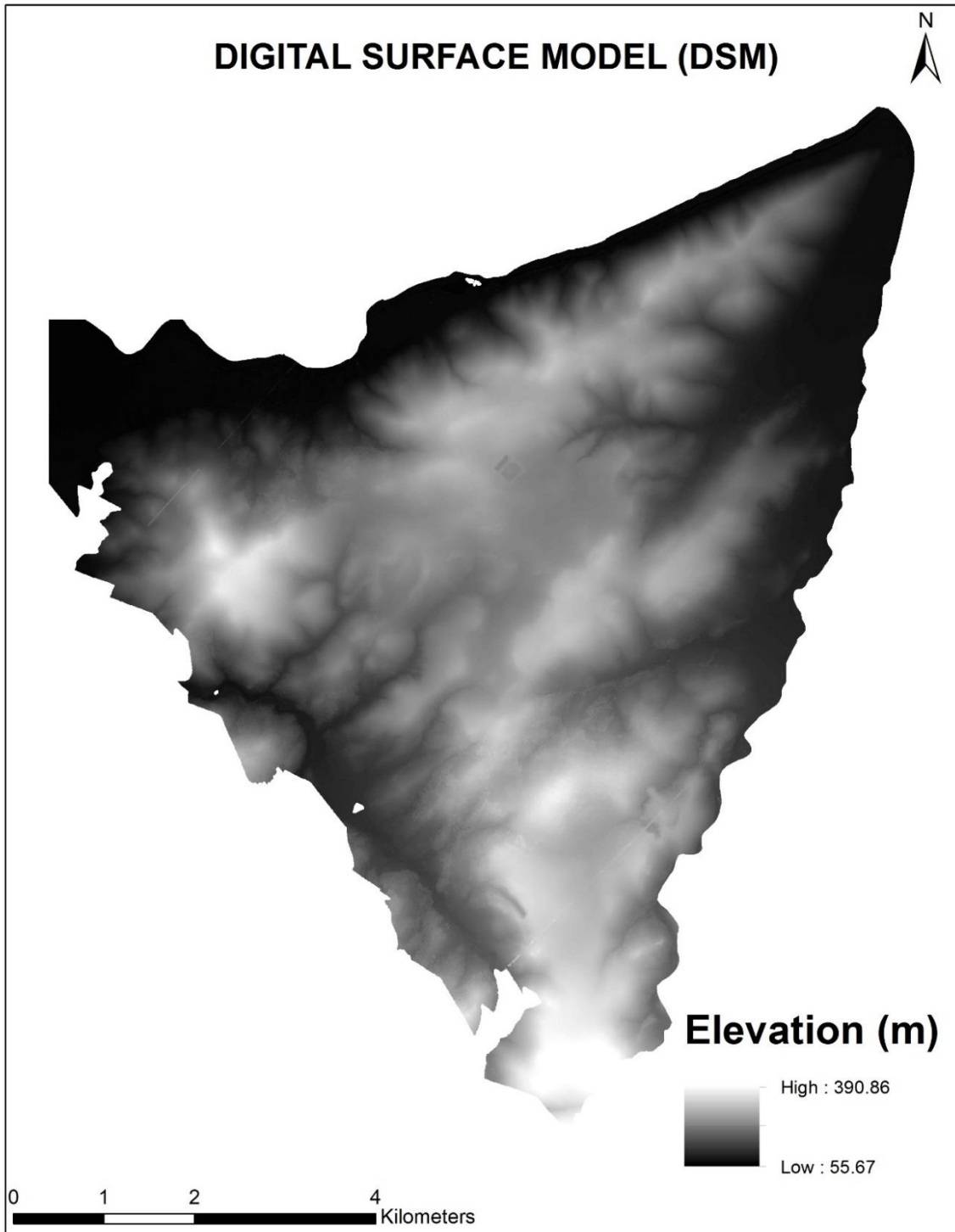
Figure 9. Digital Surface Model
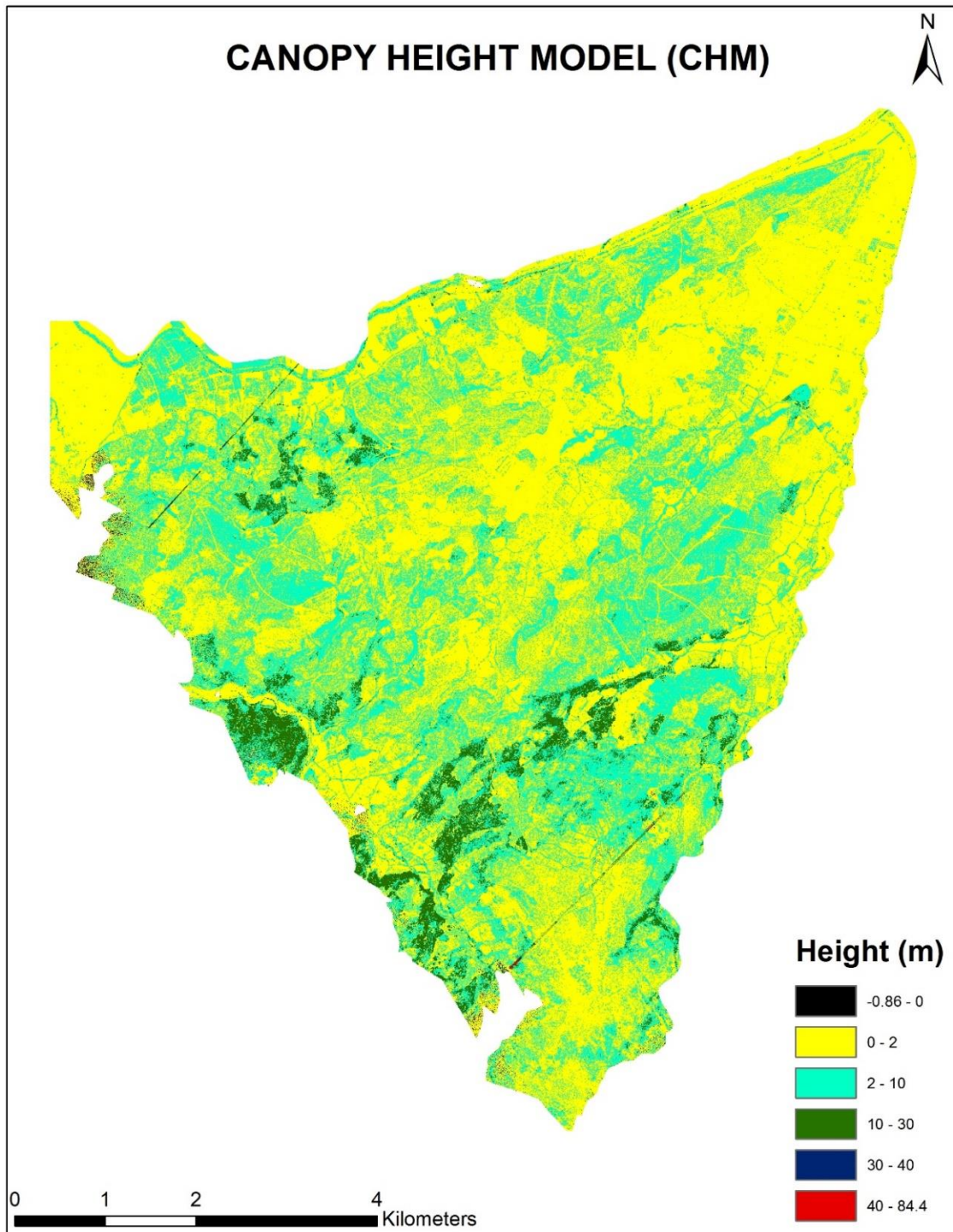
Figure 10. Canopy Height Model
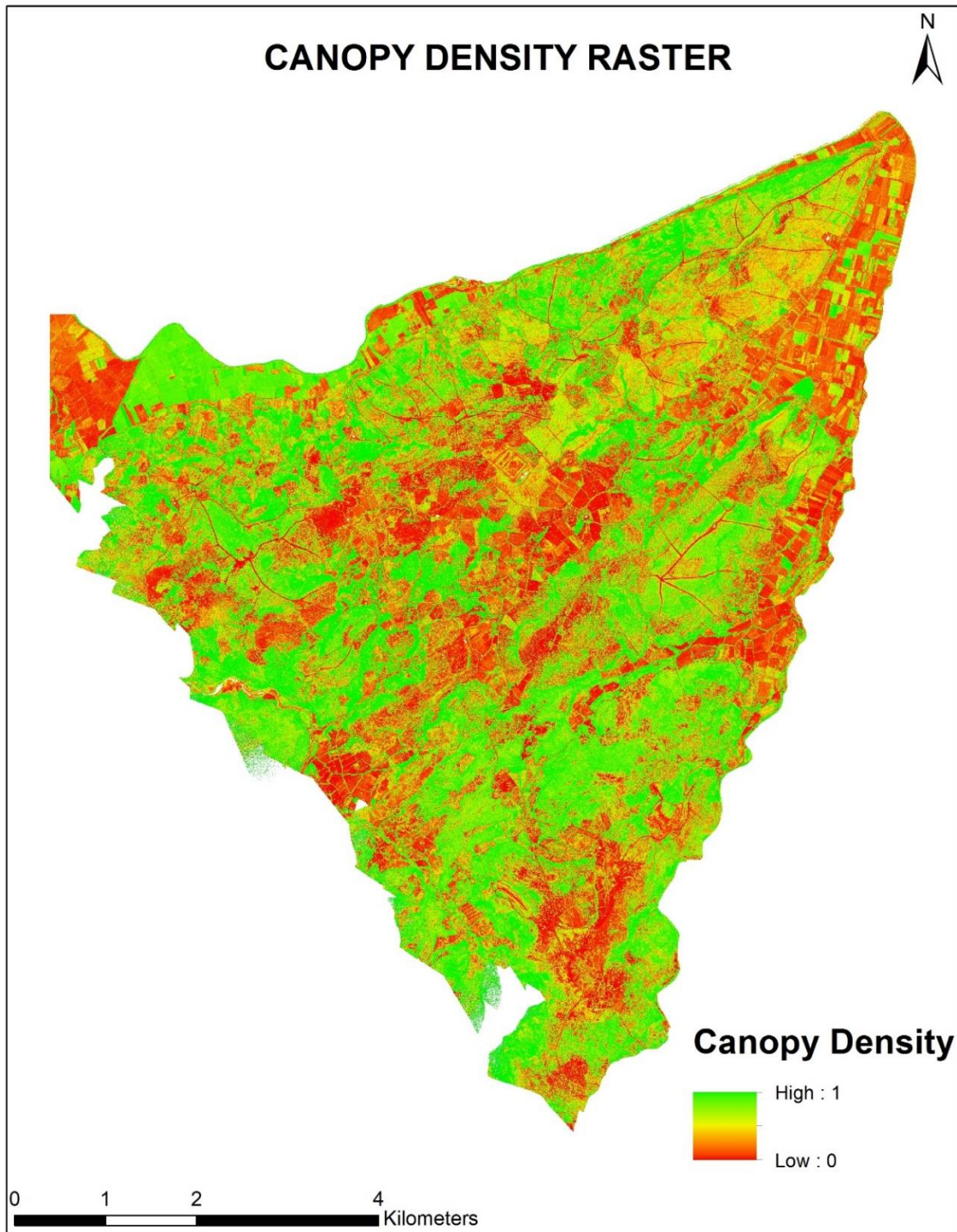
Figure 11. Canopy Density (canopy return ratio)

2.4.No Data Pixels in Processed Raster

One of the major problems incurred when working with LiDAR data processing in developing DTMs, DSM, CHMs as well as the Canopy/Biomass Density are the NoData cells in the produced raster especially when using the point to raster tool in ArcGIS. The results from this tool are quick to generate but the frequency of the NoData cells may make the raster appear noisy. This problem can be further magnified where vegetation cover is so dense that it has obscured the ground returns (Esri, 2011). It is possible to reduce this effect by post processing the raster with a Python script that incorporates the conditional function (con) in spatial analyst tool of ArcGIS. When using the Conditional evaluation function, each cell in the raster DEM is evaluated for the NoData value. If the evaluation is true, then a floating filter is used to gain the average values of the surrounding cells and applied to the NoData cell. If the evaluation is false, the original raster is used. Con (<condition>, <true expression>, <false expression>)

The NoData problem described above did not spare this study and such cases where solved using a standalone python script such as one described. Figure (12) shows a sample Python statement used for removing the NoData values in this study (URL-4, 2016):

```
Python
>>> import arcpy
from arcpy import env
from arcpy.sa import *

env.workspace="E:/THESIS_DATA/"

inRaster="E:/THESIS_DATA/1200_studyArea/DTM_1m"

arcpy.CheckOutExtension ("Spatial")

outCon=Con(IsNull(inRaster), FocalStatistics (inRaster, NbrRectangle (5,5, "CELL"), "MEAN"),
 inRaster)

outCon.save ("E:/THESIS_DATA/1200_StudyArea/outCon")
```

Figure 12. Screen shot of no data script in ArcGIS

2.5. Multiple Linear Regression Processing

Volume per hectare was estimated using multiple linear regression analysis in SPSS and Excel, with LiDAR height distributional parameters and field measurements of the plot volume used as independent and dependent variables, respectively. The field-surveyed sample plot total volume is the sum of the stem volumes of individual trees above 8 cm DBH.

The independent variables for predicting the plot volume as well as other parameters such as mean height, dominant height and number of trees were obtained from canopy height model (CHM) metrics, canopy density metrics and pixel values from WorldView-3 imagery bands. Multiple linear regression analysis was performed on each data set, with the estimated regression models subsequently evaluated in details for selection of the optimal regression model for each parameter. Finally, models exhibiting the best performance were verified with test plots.

2.6. Extraction of LiDAR Metrics and Pixel Values From WorldView3-Imagery

LiDAR height metrics were extracted from the CHM and were used as the explanatory variables of the sample plot volume together with density metrics extracted from the canopy return ratio. The height threshold for distinguishing canopy returns may differ according to the forest type and characteristics of the surveyed location (Næsset 2002; Maltamo, Hyyppä, and Malinen 2006; Chen et al. 2007). In this study, values less than 5 m were excluded to eliminate ground hits and the effect of weeds, stones, shrubs, etc. from the tree canopy datasets (cf. Næsset, 1997a; Nilsson, 1996). The 30 m as maximum threshold was used so as to get rid of noise points because no tree measured above 32 m in our study area. This was achieved by using the calculate algebra tool in spatial analyst of ArcGIS with a Set Null script specifying the required range of 5 m to 30 m. The multispectral worldview image (Figure 13) was first degraded with a scale factor of 20 for both x and y in Erdas Imaging 2010 so as to get the aggregated average pixel values (digital numbers) for each sample plot area. Later, each of the 8 multispectral bands' pixel average pixel value for each sample plot was then extracted.
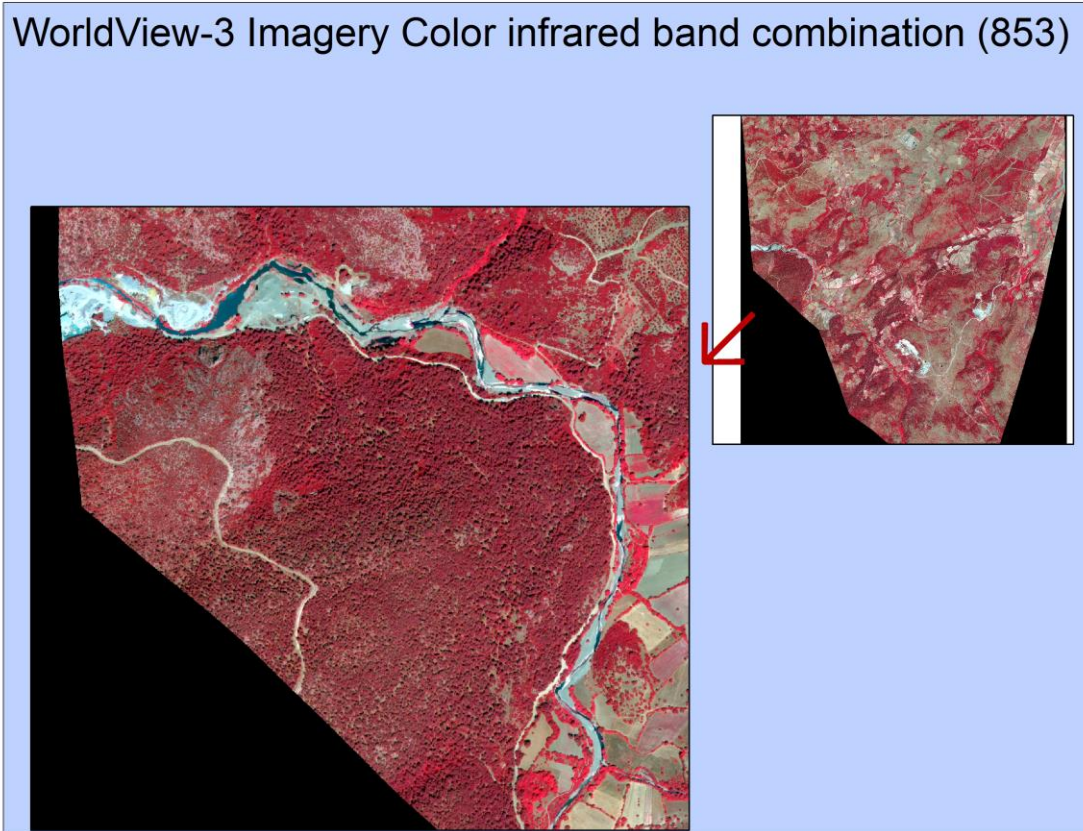
Figure 13. Multispectral Worldview-3 imagery for part of the study area (Color Infrared).

A number of metrics were derived from both the canopy height model (CHM) and the canopy return ratio. From the previous studies and experiences (Lefsky et al., 1999; Magnussen and Boudewyn, 1998; Magnussen et al., 1999; Means et al., 1999, 2000; Næsset, 1997a; Naesset and Bjerknes, 2001; Naesset & Økland, 2001; Nelson, 1997; Ziegler et al., 2000), the following metrics were derived:

From CHM;

- H_{min}, minimum of height
- H_{max}, maximum of height
- H_{range}, range of height
- H_{mean}, mean of height

- H_{std}, standard deviation of height
- H_{sum}, the sum of all heights in a sample plot
- H_{skew}, skewness of height distribution
- H_{kurt}, kurtosis of height distribution
- H_{1st}, first quartile of height distribution
- H_{2nd}, second quartile of height distribution
- H_{3rdQ}, third quartile of height distribution
- H_{ithP}, $i = 10, 20\ldots 100$ percentile height
- H_{cofv}, coefficient of variation of height
  From Canopy Return Ratio
- D_{min}, minimum of density
- D_{max}, maximum of density
- D_{range}, range of density
- D_{mean}, mean of density
- D_{sum}, sum of densities
- D_{std}, standard deviation of density
- D_{cofv}, coefficient of variation of density
  Other Parameters
- Area (A)
- Slope (S)
- Elevation (E)
- $WV3_{band1}$, pixel value for band 1
- $WV3_{band2}$, pixel value for band 2
- $WV3_{band3}$, pixel value for band 3
- $WV3_{band4}$, pixel value for band 4
- $WV3_{band5}$, pixel value for band 5
- $WV3_{band6}$, pixel value for band 6
- $WV3_{band7}$, pixel value for band 7
- $WV3_{band8}$, pixel value for band 8

Table 3. LiDAR derived metrics 1

S.P #	Area	D_{mean}	D_{Std}	D_{CofV}	H_{min}	H_{max}	H_{range}	H_{mean}	H_{std}
2	586.0	0.7	0.3	216.7	0.0	9.9	9.9	3.9	3.3
6	387.0	0.9	0.1	685.0	0.0	13.6	13.6	8.3	4.1
7	386.0	0.9	0.1	995.5	0.0	14.8	14.8	9.5	3.0
9	782.0	0.9	0.2	513.4	0.0	17.9	17.9	9.3	5.4
10	386.0	0.8	0.2	461.4	9.5	19.5	10.1	14.7	1.9
11	387.0	1.0	0.0	2237.1	0.0	16.9	16.9	11.0	4.2
21	789.0	0.8	0.2	467.3	0.0	28.7	28.7	19.5	3.8
23	588.0	0.7	0.2	448.6	0.0	21.8	21.8	14.1	2.8
24	588.0	0.9	0.2	471.4	0.0	19.8	19.8	12.6	3.9
25	784.0	0.9	0.1	871.8	0.0	21.6	21.6	11.1	6.2
26	784.0	0.8	0.1	563.1	0.0	16.0	16.0	9.4	4.6
27	392.0	0.7	0.3	280.7	0.0	14.4	14.4	5.4	4.3
28	392.0	0.9	0.1	669.7	0.0	11.3	11.3	5.5	3.8
29	391.0	0.8	0.2	474.1	0.0	8.7	8.7	4.4	3.1
30	386.0	0.9	0.2	399.5	0.0	12.3	12.3	6.1	4.2
31	385.0	0.8	0.2	486.0	0.0	13.7	13.7	8.2	3.7
32	386.0	0.9	0.1	728.4	0.0	13.4	13.4	9.0	3.1
33	588.0	0.9	0.1	927.9	0.0	11.7	11.7	5.0	3.8
35	586.0	0.8	0.2	430.1	0.0	21.5	21.5	12.4	6.6
36	785.0	0.9	0.1	823.2	0.0	19.3	19.3	13.7	4.1
37	586.0	0.8	0.1	573.9	0.0	16.7	16.7	10.1	4.4
39	391.0	0.8	0.1	955.2	0.0	14.1	14.1	9.5	2.2
40	588.0	0.9	0.2	467.1	0.0	13.7	13.7	9.1	4.2
42	586.0	0.9	0.2	505.8	0.0	19.4	19.4	12.2	4.8
43	396.0	0.8	0.1	610.1	0.0	14.7	14.7	8.6	3.9
45	793.0	0.9	0.2	410.1	0.0	9.0	9.0	0.4	1.5
46	396.0	0.6	0.2	347.2	0.0	14.7	14.7	8.4	3.5
50	798.0	0.8	0.3	294.9	0.0	9.3	9.3	1.4	2.7
52	794.0	0.8	0.2	345.6	0.0	9.2	9.2	0.5	1.7
53	796.0	0.7	0.3	254.5	0.0	9.5	9.5	2.1	3.1
54	594.0	0.8	0.2	485.8	0.0	9.7	9.7	4.3	3.4
55	396.0	0.8	0.3	312.6	6.8	16.2	9.4	13.0	1.6
57	396.0	0.9	0.2	564.3	0.0	12.6	12.6	7.1	4.0
59	585.0	0.8	0.2	450.9	0.0	21.4	21.4	14.0	3.5
60	392.0	0.8	0.1	535.1	0.0	17.8	17.8	11.4	3.3
61	784.0	0.4	0.3	137.3	0.0	10.4	10.4	0.7	2.2
62	194.0	0.9	0.1	1052.3	0.0	19.0	19.0	8.4	3.7
63	588.0	0.9	0.1	1116.5	0.0	19.1	19.1	8.9	6.0
65	786.0	0.7	0.2	295.4	0.0	17.7	17.7	7.0	4.7
66	786.0	0.9	0.2	451.3	0.0	12.0	12.0	3.9	4.0

Table 4. LiDAR derived metrics 2

S.P #	H_{sum}	H_{CofV}	Skewness	Kurtosis	H_{1stQ}	H_{median}	H_{3rdQ}	$H_{10th P}$	H_{20thP}
2	2280.6	116.9	-1.7	7.4	5.0	6.0	7.0	5.0	5.0
6	3222.3	202.5	-1.1	5.1	7.0	9.0	10.0	6.0	7.0
7	3665.2	312.6	-1.0	5.1	8.0	9.0	11.0	6.0	7.6
9	7277.1	171.7	-0.6	3.5	8.0	11.0	13.0	6.0	7.0
10	5670.9	793.9	0.1	3.0	13.0	14.0	15.0	11.0	12.0
11	4274.4	261.4	-0.8	4.1	8.0	11.0	12.0	6.0	8.0
21	15373.9	511.6	-0.9	4.7	16.0	19.0	21.0	13.0	15.0
23	8307.0	500.3	-0.6	4.6	11.0	13.0	15.0	10.0	11.0
24	7430.4	325.6	-0.4	3.5	9.0	12.0	14.0	7.0	9.0
25	8659.7	177.6	-0.2	2.4	7.0	11.0	15.0	5.0	6.8
26	7338.4	203.3	-0.8	3.9	8.0	10.0	12.0	6.0	7.0
27	2102.5	125.0	-0.4	4.2	6.0	7.0	9.0	5.0	5.2
28	2142.3	142.2	-0.6	5.2	6.0	7.0	8.0	5.0	5.4
29	1708.0	142.6	-1.0	2.6	5.0	5.0	6.0	0.0	0.0
30	2340.0	144.6	-1.0	4.8	6.0	7.0	9.0	5.0	6.0
31	3173.9	225.1	-1.0	4.5	6.8	8.0	10.0	5.0	6.0
32	3459.0	293.1	-1.2	5.4	7.0	9.0	10.0	6.0	7.0
33	2936.2	132.2	-0.9	4.5	5.0	6.0	8.0	5.0	5.0
35	7261.1	189.2	-1.0	4.5	12.0	14.0	16.0	9.0	11.0
36	10738.7	332.9	-1.2	4.8	10.0	13.0	16.0	8.0	10.0
37	5939.7	228.6	-0.6	4.1	8.0	10.0	12.0	6.0	8.0
39	3726.0	440.2	-1.1	6.4	8.0	9.0	11.0	7.0	7.6
40	5374.4	218.9	-0.9	3.2	6.0	8.0	11.0	4.0	6.0
42	7157.7	256.0	-0.7	3.8	10.0	13.0	15.0	8.0	9.0
43	3389.2	222.2	-0.9	5.3	8.0	9.0	10.0	6.0	7.0
45	306.9	25.8	-1.3	4.6	5.0	5.0	6.0	3.0	5.0
46	3308.8	236.3	-0.6	4.0	7.0	9.0	10.0	5.0	6.0
50	1136.8	52.3	-1.5	5.0	5.0	6.0	7.0	4.0	5.0
52	382.1	29.2	-1.3	6.0	5.0	5.0	6.0	5.0	5.0
53	1694.7	69.3	-1.4	4.9	5.0	6.0	7.0	4.5	5.0
54	2543.2	124.8	-1.4	5.7	5.0	6.0	7.0	5.0	5.0
55	5131.4	833.2	-0.4	3.2	11.0	12.0	14.0	10.0	11.0
57	2802.5	177.4	-1.1	5.1	6.0	8.0	9.0	5.0	6.0
59	8163.4	396.0	-0.3	3.0	11.0	13.0	15.0	8.0	10.0
60	4472.4	342.7	-0.4	3.3	9.0	11.0	13.0	6.6	8.0
61	557.7	32.4	-1.1	7.4	5.0	6.0	7.0	5.0	5.0
62	1632.2	230.4	-0.1	4.7	6.0	8.0	10.0	6.0	6.0
63	5242.6	149.4	-0.4	3.4	9.0	11.0	13.0	6.0	8.0
65	5532.6	149.9	0.0	3.7	6.0	8.0	10.0	5.0	6.0
66	3072.9	96.8	-0.7	5.0	6.0	7.0	8.0	5.0	5.0

Table 5. LiDAR derived metrics 3 except for slope derived from contour maps

S.P #	H_{30thP}	H_{40thP}	H_{50thP}	H_{60thP}	H_{70thP}	H_{80thP}	H_{90thP}	H_{100thP}	Elevation	Slope
2	5.0	5.0	6.0	6.0	6.0	7.0	7.0	9.0	176.7	18.0
6	8.0	9.0	9.0	10.0	10.0	11.0	12.0	13.0	110.7	32.0
7	8.0	9.0	9.0	10.0	11.0	11.0	12.0	14.0	186.9	25.0
9	9.0	10.0	11.0	11.0	12.0	13.0	15.0	17.0	112.7	15.0
10	13.0	13.0	14.0	14.0	15.0	15.0	16.4	19.0	169.9	14.0
11	9.0	10.0	11.0	10.0	11.0	11.0	12.0	14.0	119.6	5.0
21	17.0	18.0	19.0	20.0	21.0	22.0	23.0	28.0	145.9	23.0
23	12.0	13.0	13.0	14.0	15.0	15.0	16.0	21.0	175.2	15.0
24	10.0	11.0	12.0	13.0	13.0	14.0	16.0	19.0	166.6	25.0
25	8.0	10.0	11.0	11.0	12.0	13.0	14.0	16.0	171.8	5.0
26	8.0	9.0	10.0	11.0	11.0	12.0	13.0	15.0	263.3	22.0
27	6.0	7.0	7.0	8.0	9.0	9.0	10.9	14.0	224.8	25.0
28	6.0	7.0	7.0	7.0	8.0	9.0	9.0	11.0	254.1	15.0
29	5.0	5.0	5.0	6.0	6.0	6.0	7.0	8.0	180.5	15.0
30	6.0	7.0	7.0	8.0	8.0	9.6	10.0	12.0	223.8	15.0
31	7.0	8.0	8.0	13.0	15.0	16.0	18.0	21.0	130.8	5.0
32	7.0	8.0	9.0	9.0	10.0	10.0	11.0	13.0	124.6	34.0
33	5.0	6.0	6.0	7.0	7.0	8.0	9.0	11.0	309.9	15.0
35	12.0	13.8	14.0	15.0	16.0	16.0	18.0	21.0	168.4	15.0
36	11.0	12.2	13.0	14.0	15.0	16.0	17.0	19.0	235.3	31.0
37	8.0	9.0	10.0	11.0	12.0	13.0	13.4	16.0	268.7	5.0
39	8.0	9.0	9.0	10.0	10.0	11.0	12.0	14.0	241.5	15.0
40	7.0	7.2	8.0	9.0	10.0	10.0	11.0	13.0	237.2	38.0
42	11.0	11.0	13.0	14.0	15.0	15.0	16.0	19.0	158.2	35.0
43	8.0	8.0	9.0	9.8	10.0	11.0	12.0	13.0	217.3	25.0
45	5.0	5.0	5.0	5.0	6.0	6.8	7.4	8.0	223.7	8.0
46	7.0	8.0	9.0	9.0	10.0	11.0	12.0	14.0	174.7	5.0
50	5.0	5.0	6.0	10.0	10.0	11.0	11.0	14.0	379.0	5.0
52	5.0	5.0	5.0	5.0	6.0	6.0	7.0	9.0	329.5	30.0
53	5.0	5.0	6.0	6.0	7.0	7.0	8.0	9.0	353.2	15.0
54	5.0	6.0	6.0	6.0	7.0	7.0	8.0	9.0	364.7	16.0
55	11.0	12.0	12.0	13.0	13.0	14.0	14.0	16.0	176.7	5.0
57	7.0	7.0	8.0	6.6	7.0	7.0	8.0	9.0	237.5	25.0
59	11.5	12.0	13.0	14.0	15.0	16.0	17.0	21.0	143.5	15.0
60	9.0	10.0	11.0	12.0	13.0	14.0	15.0	17.0	154.6	20.0
61	6.0	6.0	6.0	7.0	7.0	7.8	8.0	10.0	171.3	34.0
62	7.0	7.2	8.0	9.0	10.0	10.4	11.7	18.0	170.8	27.0
63	9.0	10.0	11.0	12.0	13.0	14.0	15.0	19.0	253.1	25.0
65	7.0	7.0	8.0	9.0	9.0	10.0	10.0	12.0	246.2	13.0
66	6.0	6.0	7.0	7.0	8.0	8.2	10.0	12.0	289.6	25.0

Table 6. WorldView-3 pixel values for each band

S.P. #	WV3$_{band1}$	WV3$_{band2}$	WV3$_{band3}$	WV3$_{band4}$	WV3$_{band5}$	WV3$_{band6}$	WV3$_{band7}$	WV3$_{band8}$
2	232	202	252	237	130	358	445	414
6	228	188	225	202	111	309	390	359
7	224	185	222	195	104	317	408	373
9	234	200	243	231	138	329	422	392
10	225	186	217	193	107	292	369	337
11	226	185	217	190	103	290	391	346
21	225	188	221	196	107	286	346	324
23	227	192	224	204	118	277	320	307
24	226	190	224	201	111	299	366	348
25	228	194	233	210	115.5	313	392	375
26	231	200	240	227	137	322	380	367
27	229	196	233	219	129	305	368	356
28	227	193	228	207	115	304	370	355
29	227	193	229	208	110	317	402	377
30	235	206	247	236	144	312	374	359
31	228	194	226	206	109	300	370	350
32	228	196	232	211	112	318	422	400
33	225	190	223	203	110	300	367	349
35	228	193	224	200	110	276	332	318
36	226	191	229	206	115	308	372	353
37	225	189	220	197	109	284	340	317
39	225	188	221	199	109	284	341	327
40	228	193	222	200	106	290	367	349
42	228	196	231	213	116	314	392	369
43	223	187	214	189	98	270	323	308
45	228.5	192.5	230.5	210	118	338	440	410.5
46	225	188	227	200	108	297	353	325
50	222	188	220	199	110	305	386	375
52	236	211	259	253	158	340	401	388
53	230	201	243	234	139	323	379	375
54	223	189	226	207	115	308	376	364
55	225	187	216	190	99	277	233	311
57	224	190	219	199	106	277	329	317
59	226	190	222	200	102	295	372	348
60	230	196	231	214	124	299	357	349
61	226	192	221	201	109	295	379	365
62	229	196	236	210	115	321	390	365
63	225	187	216	192	105	289	362	349
65	227	192	227	208	118	291	342	326
66	226	191	225	210	118	313	386	375

2.7. Multiple Linear Regression Analysis

2.7.1. Independent Variable Selection

Multiple linear regression modelling was performed using the field-measured sample plot volume as a dependent variable and LiDAR height metrics and pixel values of bands from WorldView-3 image as independent variables. Not every variable was used to model sample plot volume, stem number, mean height and dominant height as this might be inefficient and unreliable because the effects of each parameter is different. Stepwise, backward as well as forward selection methods in SPSS were used to eliminate some variables.

However, variables selected by these selection methods might have a linear dependency relationship, which is a phenomenon referred to as multicollinearity (Kwak et al., 2014). Thus, some variables selected by stepwise/backward selection might have a linear dependency relationship, which is a phenomenon referred to as multicollinearity. This multicollinearity between selected independent variables must be evaluated using a variance inflation factor (VIF), calculated by the formula shown as equation (2) (O'Brien 2007).

$$\text{VIF} = \frac{1}{1-R_n^2} \qquad \text{Eq. 2}$$

where R_n^2 is the coefficient of determination when a regression analysis is performed with the dependent variable, y , and independent variables, $x_1, x_2, x_3, \ldots, x_{n-1}$. AVIF < 10 is suitable for selecting independent variables, but values above this indicate multicollinearity (Kutner et al. 2004). This procedure was used in this study in eliminating multicollinearity between independent variables.

2.7.2. Model Selection

A multiple linear regression analysis was done as shown in equation (3) using combinations of the selected variables derived from LiDAR data and WorldView-3 imagery as independent variables.

$$y = \alpha + \beta_1 x_1 + \beta_2 x_2 + \beta_3 x_3 + \cdots + \beta_n x_n, \quad \text{Eq. 3}$$

where y is the sample plot volume(m³/ha)/stem number/dominant/mean height surveyed in the field; x_1, ; x_2, ; x_3, ….; x_n are the selected LiDAR metric variables as well as pixel values from WorldView-3 bands; α is the intercept/constant and β_1, β_2, β_3, …, β_n are the regression coefficients.

Different regression models with various combinations of selected variables can be assessed by their R^2, adjusted R^2, root mean square error (RMSE), sum of square error (SSE), AIC, Mallow's Cp, and Bayesian information criterion (BIC) values (SAS 2006). The coefficient of determination, R^2, provides a measure of how well future outcomes are likely to be predicted by the model without considering the number of independent variables (Kvålseth 1985). Therefore, the fitness assessment between regression models must be conducted using the adjusted R^2 value, which adjusts for the number of explanatory terms in a model. The adjusted R^2 together with RMSE where used as the basis for selecting suitable models in this study.

The Root Mean Square Error (RMSE) (also called the root mean square deviation, RMSD) is a frequently used measure of the difference between values predicted by a model and the values actually observed from the environment that is being modelled. These individual differences are also called residuals, and the RMSE serves to aggregate them into a single measure of predictive power. It is calculated using the equation 4 below;

$$RMSE = \sqrt{\frac{\sum_{i=1}^{n}(X_{obs,i} - X_{model,i})^2}{n}} \qquad \text{Eq. 4}$$

3. Results

In the first phase, mean height, dominant height, stem number and volume of 30 sample plots were regressed against the predictor variables derived from the height distribution metrics of canopy height model (CHM) and the density distribution metrics of the canopy return ratio. The second phase had both LiDAR metrics and WorldView3 imagery pixel values for each band as independent variables. Each dependent variable was regressed against the metrics as described above in SPSS and Microsoft Excel. From the 40 sample plots, random numbers were created and the first 30 sample plots were taken as model training sample plots and the last 10 taken as model test plots. This was repeated each time regression was performed for all the dependent variables i.e. volume, number of stems, mean height and dominant height. The p-value for each independent variable to be significant was set to be 0.05 or less otherwise its discarded. Also the presence of collinearity in the regression analysis was assessed by way of analyzing the variance inflation factor (VIF) every time the multiple regression was run in SPSS. Regression models with independent variables showing VIF of greater than 10 (VIF< 10) were discarded there and then as this indicate the presence of collinearity. Some of the models initially suggested by the stepwise selection procedure were subject to serious collinearity. The models selected for further analysis were therefore those indicated by the stepwise procedure that fulfilled the requirement of VIF< 10. Collinearity was observed especially for height distribution metrics from the CHM such as the quartiles and the percentiles.

3.1. Dominant Height

After running the regression analysis in SPSS repeatedly with observed dominant height as the dependent variable and all the height and density metrics as independent variables, the best model was selected. This was arrived at, just like in other models, after conducting a thorough analysis of the other regression models produced. It had the adjusted coefficient of determination (R^2) of 0.83 as well as a root meet square error (RMSE) of 1.78 m. Only two independent variables for this regression model were involved; the third quartile

of heights (H_{3rdQ}) and the tenth percentile of heights (H_{10thP}). Figure (14) shows the scatter plots of the predicted dominant height using the regression model produced against the field observed dominant height for the ten test sample plots while table (7) shows the model regression statistics.
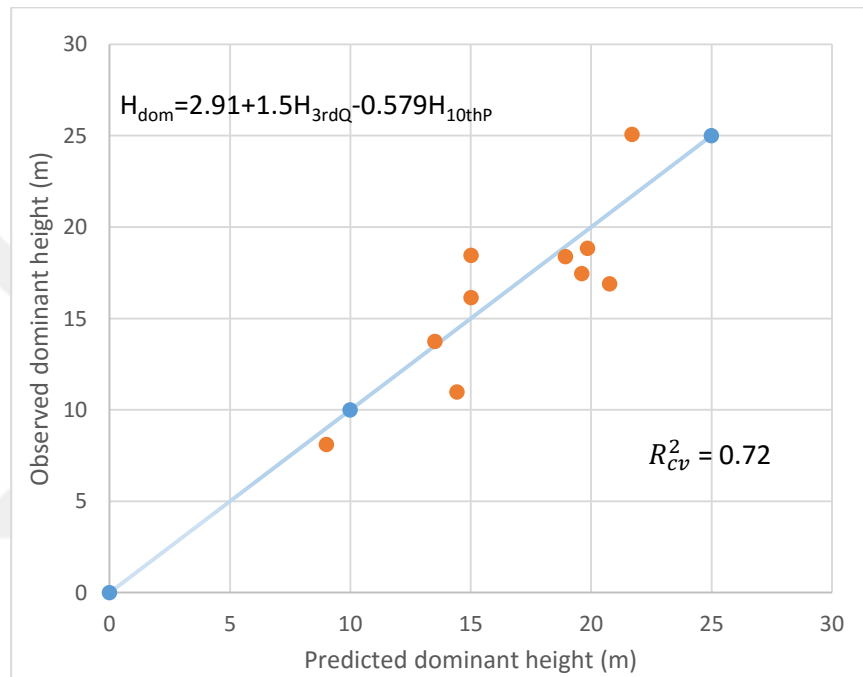

Figure 14. Scatterplots of predicted against observed dominant height

When only third quartile of height (H_{3rdQ}) was used as independent variable, while the observed dominant height as dependent variable as was the case in one analysis, the resultant model had an adjusted R^2 of 0.78 and a root mean square error (RMSE) of 2.07 m. This was not so different from the selected regression model for dominant height only that with the addition of the 10th percentile of height, the adjusted R^2 as well as the RMSE were adjusted a bit.

Table 7. Dominant height regression model output

Regression Statistics					
Multiple R	0.918				
R Square	0.843				
Adjusted R Square	0.831				
Standard Error	1.881				
Observations	30				
ANOVA					
	df	*SS*	*MS*	*F*	*Significance F*
Regression	2	512.591	256.295	72.420	0.000
Residual	27	95.554	3.539		
Total	29	608.145			
	Coefficients	*Standard Error*	*t Stat*	*P-value*	
Intercept	2.909	1.114	2.612	0.015	
3rd Q	1.500	0.178	8.448	0.000	
10th P	-0.579	0.262	-2.207	0.036	

The regression statistics for this model shows that about 84% of the variation in the estimation of dominant height can be attributed to the third quartile of heights (H_{3rdQ} and the tenth percentile of the height (H_{10thP}). Analysis of variance (ANOVA) shows a great significance of F (p-value = 0.000) indicating that the probability of the regression output being random or by chance is very slim. The p-values for the explanatory variables are also very significant giving the reliability of the regression's y-intercept and the coefficients for the independent variables. Also the residual scatterplot as shown in figure (15) has no pattern and revolves around zero, signs that the model is output is not random.
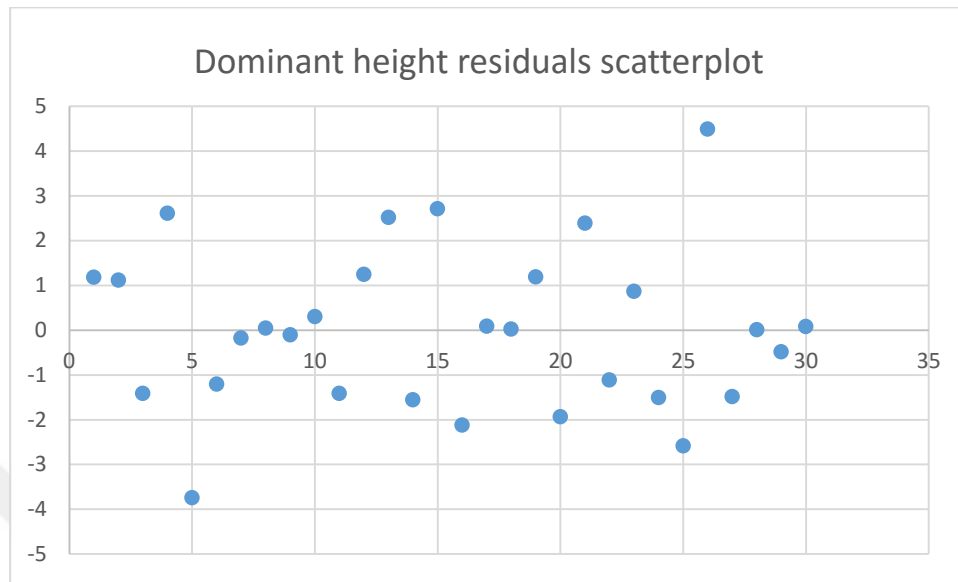
Figure 15. Residual scatterplots for dominant height

3.2. Average Height

For average height, the best regression model selected had the adjusted coefficient of determination (R^2) of 0.83 and a root mean square error (RMSE) of 1.68metres. The independent variables that were used in this regression model were the mean density (D_{mean}), the density coefficient of variation (D_{cofv}) and the third quartile deviation (H_{3rdQ}). Figure (16) and table (8) show the scatter plots of the predicted average height against the observed field average height for the ten test sample plots and the regression statistics respectively.

$$H_{average}=7.64-10.11D_{mean}+0.0036D_{cofv}+1.14H_{3rdQ}$$
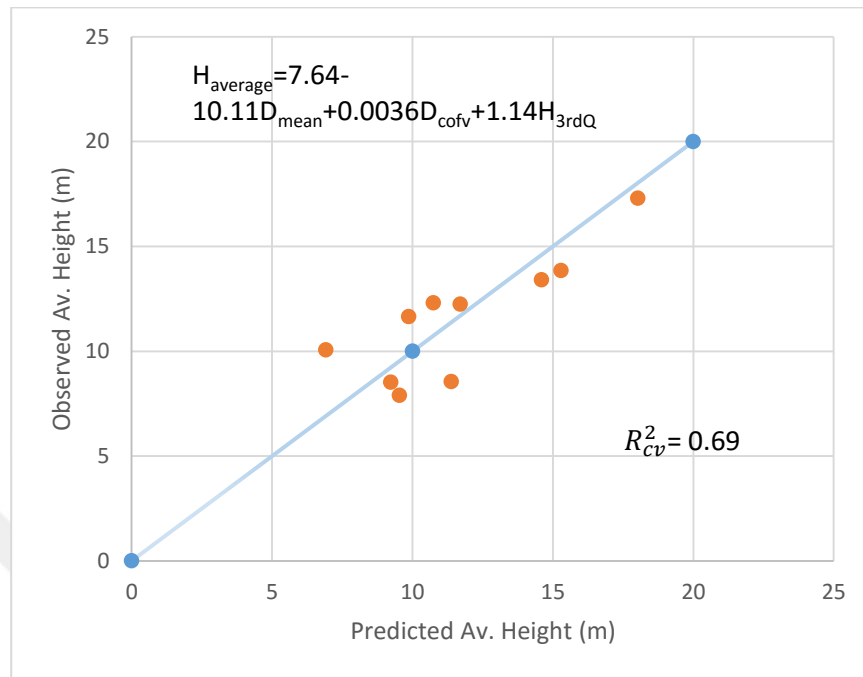
$$R^2_{cv}= 0.69$$

Figure 16. Scatterplots of predicted against observed average height

The closest regression output to this selected model for plot average height had an adjusted R^2 of 0.812 and a root mean square error (RMSE) of 1.90metres. This regression output had independent variables as density coefficient of variation (D_{cofv}) and height third quartile (H_{3rdQ}) only. Again this goes to show that the addition of the mean density (D_{mean}) in the case of the selected model for average height plays a role as there is an increase in the adjusted R^2 and also a reduction in the RMSE.

Table 8. Average height regression output

Average height Regression Statistics					
Multiple R	0.921				
R Square	0.849				
Adjusted R Square	0.831				
Standard Error	1.808				
Observations	30				
ANOVA					
	df	SS	MS	F	Significance F
Regression	3	477.698	159.233	48.698	0.000
Residual	26	85.015	3.27		
Total	29	562.712			
	Coefficients	Standard Error	t Stat	P-value	
Intercept	7.641	3.02	2.53	0.018	
D mean	-10.109	4.3	-2.351	0.027	
D CofV	0.004	0.001	3.227	0.003	
3rd Q	1.144	0.1	11.398	0.000	

The regression statistics for this model shows that about 85% of the variation in the estimation of average height can be explained by the mean density (D_{mean}), density coefficient of variation (D_{cofv}) and the third quartile of height (H_{3rdQ}). Analysis of variance (ANOVA) shows a great significance of F (0.000) indicating that the probability of the regression output being random or by chance is very slim. Again p-values for explanatory variables are also very significant giving the reliability of the regression's y-intercept and the coefficients for the independent variables. Also the residual scatterplot as shown in figure (17) has no pattern and revolves around zero.
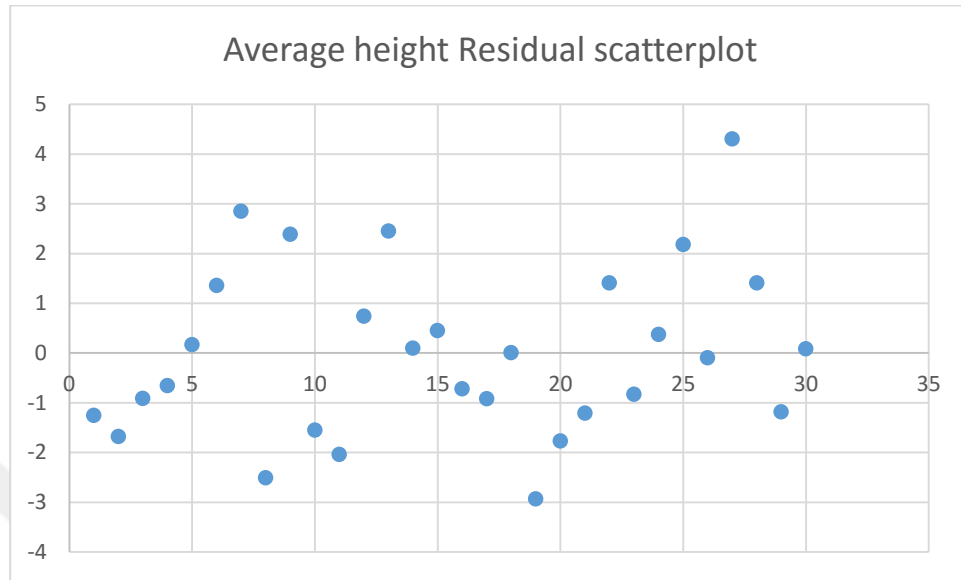
Figure 17. Residual scatterplots for average height

3.3. Number of Stems

The number of trees/stems per hectare regression models gave a highest adjusted coefficient of determination (R^2) of 0.73 and a root mean square error of 108.9 trees. The independent variables selected in this regression model were Area (A), density standard deviation (D_{std}), height first quartile (H_{1stQ}) and height twentieth percentile (H_{20thP}). Figure (18) shows the scatter plots of the predicted stem number per hectare against the field observed stem number per hectare for the ten random test sample plots while table (9) shows the model regression statistics.
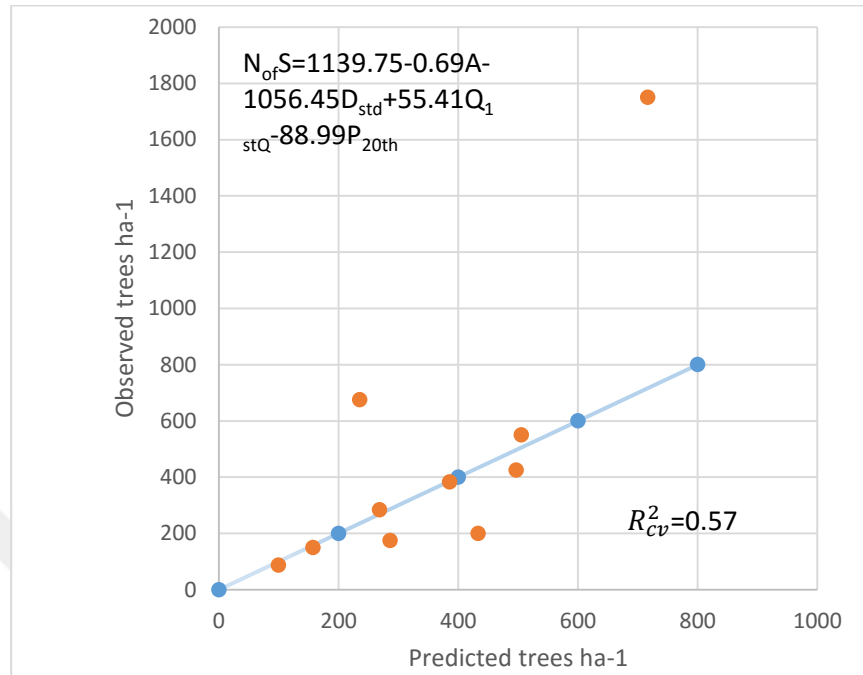
Figure 18. Scatterplots of predicted against observed trees per hectare

The other two regression outputs of interest for stem number had adjusted R^2s of 0.599 and 0.595 and root mean square errors (RMSE) of 204 trees and 121 trees respectively. The first regression output model had Area (A) and 20th percentile height (H_{20thP}) as its explanatory variables while the second had Area (A) and maximum height (H_{max}) as its explanatory variables. Despite their adjusted R^2s being almost similar, the second model predicted better though both models had negative predictions.

Table 9. Trees per hectare regression output

Number of stems Regression Statistics					
Multiple R	0.876				
R Square	0.768				
Adjusted R Square	0.731				
Standard Error	119.277				
Observations	30				
ANOVA					
	df	SS	MS	F	Significance F
Regression	4	1175241.853	293810.5	20.652	0.000
Residual	25	355672.499	14226.9		
Total	29	1530914.352			
	Coefficients	Standard Error	t Stat	P-value	
Intercept	1139.752	115.567	9.862	0.000	
AREA	-0.691	0.142	-4.877	0.000	
D Std	-1056.446	400.123	-2.64	0.014	
1st Q	55.414	24.881	2.227	0.035	
20thP	-88.991	24.104	-3.692	0.001	

The regression statistics for this model shows that about 77% of the variation in the estimation of stem number can be explained by the Area (A), density standard deviation (D_{std}), height first quartile (H_{1stQ}) and the 20th percentile of height (H_{20thP}). Analysis of variance (ANOVA) shows a great significance of F (0.000) indicating that the probability of the regression output being random or by chance is very slim. The P-values are also very significant giving the reliability of the regression's y-intercept and the coefficients for the independent variables. Also the residual scatterplot as shown in Figure 19 has no pattern and revolves around zero.
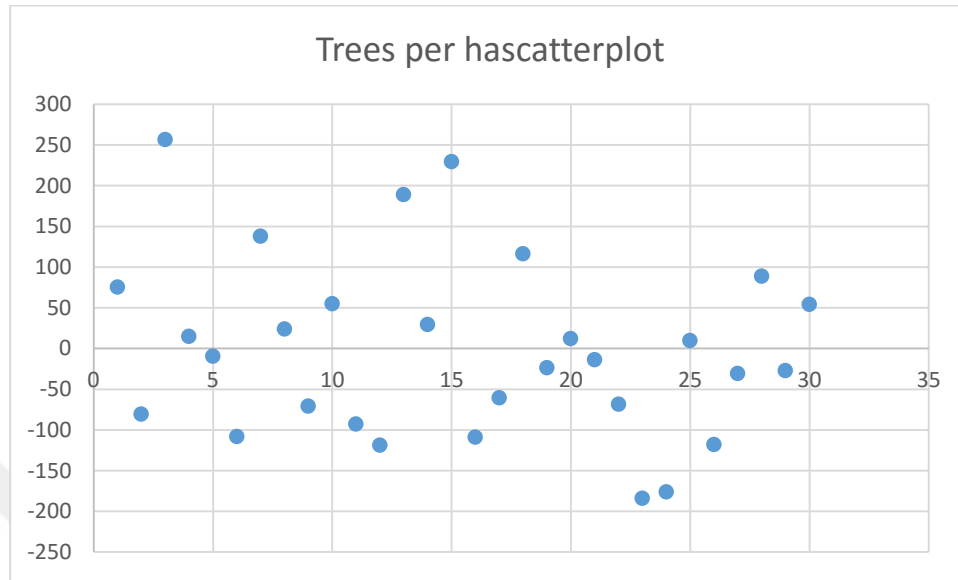
Figure 19. Residual scatterplots of trees per hectare

3.4. Volume Regression Models by LiDAR Metrics

Observed field volume per hectare was regressed against all the LiDAR distribution metrics and including the area, average slope and elevation for each sample plot. Using the stepwise and backward selection methods in SPSS, a number of regression models were obtained. Most of them gave a very high adjusted R square but their explanatory variables could not pass the p-value test (at 0.05) and also the collinearity test (at VIF < 10). There were cases where independent variables such as area, mean density, maximum height, height skewness, height kurtosis, height third quartile, height percentiles of 10th, 20th, 40th, 70th, 80th, 100th and elevation could be selected in the backward method and all of them with a very low f significance value way below 0.05 with adjusted R squared of around 90 but with so much collinearity in them. For example the 100th percentile, the maximum height and the 80th percentiles were strongly correlated and this is because the 100th percentile indicates the top height of the tallest tree in a plot and so do the maximum height and partly the 80th percentile. The third quartile was also highly correlated with these high percentiles and the same thing applied to lower quartiles and their lower percentile counterparts respectively. After conducting a number of regression models whilst varying the training sample plots and testing

sample plots by way of randomly selecting them, some models showed better performance in RMSE and adjusted R^2 and also satisfying the below 10 threshold for the VIF. Three regression models were selected with only mean height and sum of heights as independent variables in them. Also one regression model with density coefficient of variation and height coefficient of variation as its independent variables was selected. These models were picked not only on the basis of satisfying the conditions of non collinearity but also their capability to do reasonable predictions when run on test sample plots. Their adjusted coefficient of determination (R^2) ranged from 0.55 as smallest and 0.66 as highest while their RMSE ranged from 38.39 $m^3\,ha^{-1}$ as smallest and 43.74 $m^3\,ha^{-1}$ as highest. Figures (20, 21 22 and 23) show the scatter plots of models 1 to 4 with predicted volume per hectare against field calculated volume per hectare for ten random test sample plots for the four selected models.
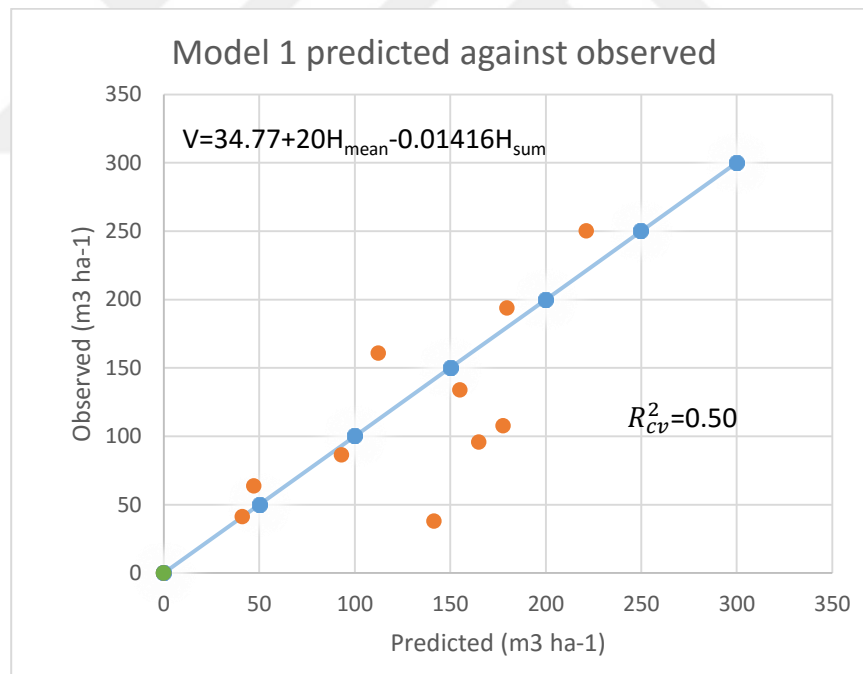

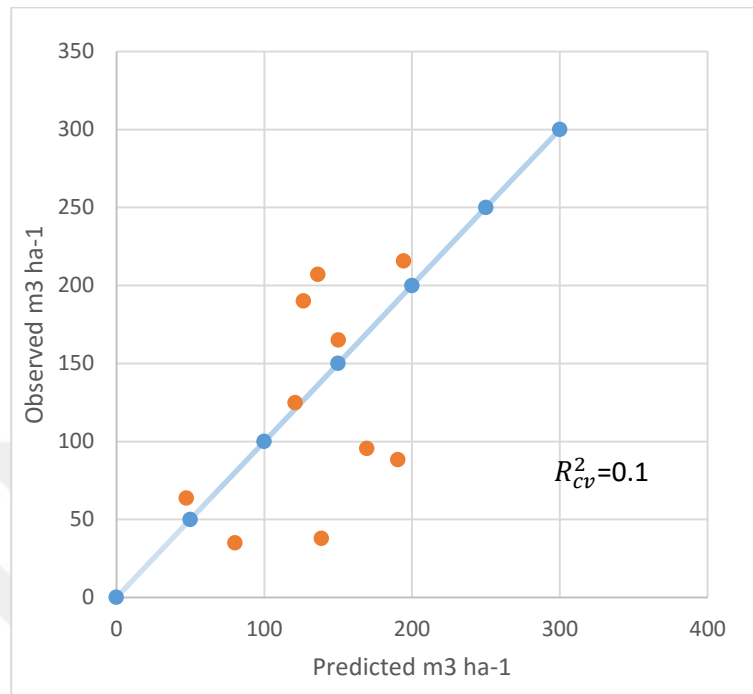Figure 20. Predictd against Observed volume for model 1

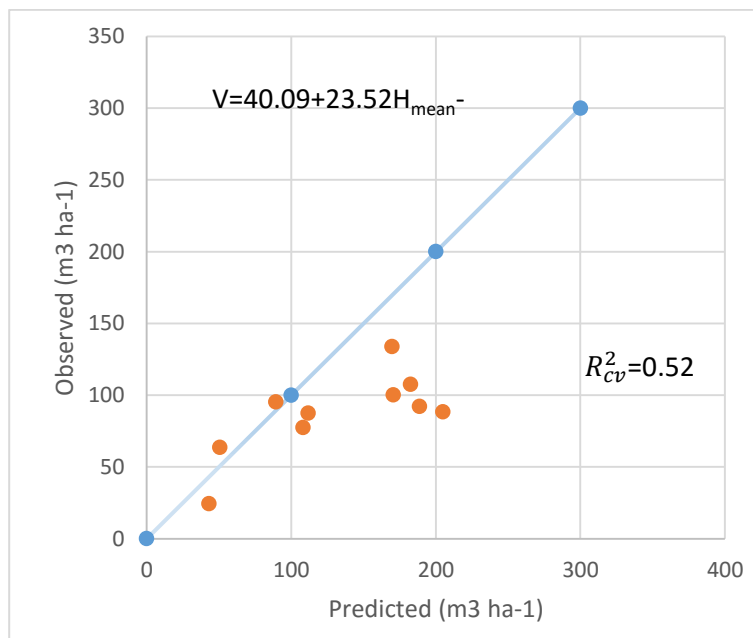Figure 21. Predicted against observed volume for model 2

Figure 22. Predicted against Observed volume for model 3

$$V=39.34+0.0538D_{cofv}+0.2558H_{cofv}$$
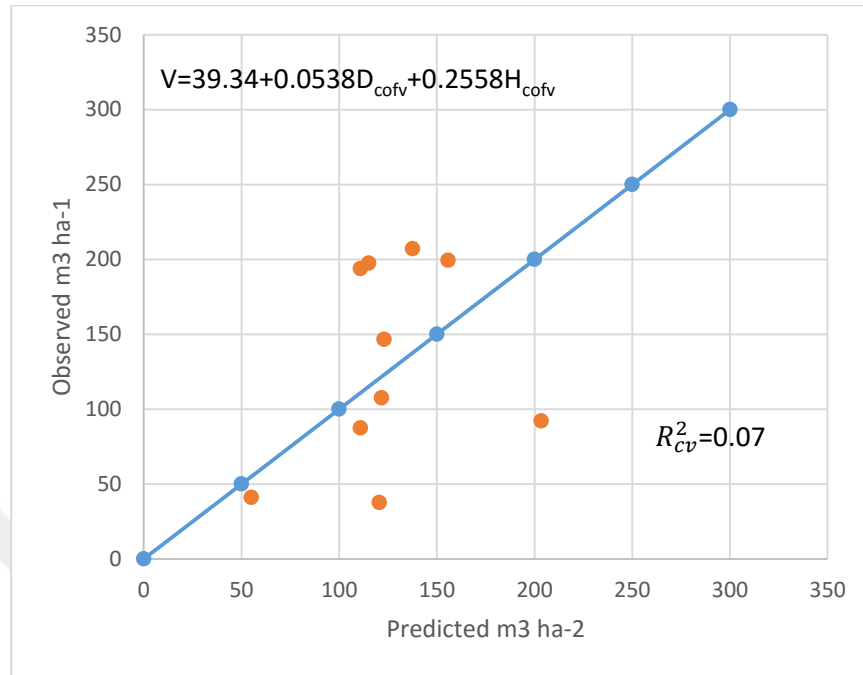
$R^2_{cv}=0.07$

Figure 23. Predicted against Observed volume for model 4

The four selected regression models for volume were analyzed in detail. Model 1 had adjusted R^2 of 0.56 and a RMSE of 43.53 m^3 ha^{-1}. The scatterplot for the residual values were normal with no clear pattern and all revolving around zero. When run on test sample plots, the model indicated better prediction power with a cross-validated R^2 of 0.50 and RMSE of 49.67 m^3 ha^{-1}. The significance of F was excellent and all p-values for explanatory variables were far below the 0.05. Both the explanatory variables had their variance inflation factors (VIF) of 3.8 which is way below the threshold of 10 indicating the there was no collinearity in them. Model 2 was the best performing model in terms of its adjusted R^2 (0.66) and a lower RMSE of 38.39 m^3 ha^{-1}. However, when run on the ten test sample plots the predictions were poor with cross-validated R^2 of 0.19 and RMSE of 61.75 m^3 ha^{-1}, the variations were not that bad as can be seen in figure (21). The scatterplot as in figure (24) for the residual values were normal with no clear pattern and all revolving around zero. The significance of F and all p-values were excellent. Both the explanatory variables had their variance inflation factors (VIF) of 4.1 indicating that there was no collinearity between them. Model 3 which was the second best performing model in terms of its adjusted R^2 (0.62) and a second lower RMSE of

41.73 m^3 ha^{-1} came out to be the best when run on test sample with cross-validated R^2 of 0.52 and a RMSE of 60.7 m^3 ha^{-1}. Of the ten predictions, 8 were over predicted with the highest being 116 m^3 ha^{-1} and only two were under predicted with very low values of 6 m^3 ha^{-1} and 13 m^3 ha^{-1} respectively. The scatterplot of the residual values were normal with no clear pattern and all revolving around zero as shown in figure (24). The significance of F and all p-values were excellent. Both the explanatory variables had their variance inflation factors (VIF) of 4.1 indicating that there was no collinearity between them. Model 4 had the adjusted R^2 of 0.57 and a RMSE of 43.74 m^3 ha^{-1}. The results were very poor when run on test plots with cross-validated R^2 of 0.07. However the model is credible as indicated by its significance of F (0.000) as well as very low p values and scatterplot of residuals.

Table 10. Model 1 regression output

Model 1 Regression Statistics					
Multiple R	0.768				
R Square	0.59				
Adjusted R Square	0.56				
Standard Error	45.882				
Observations	30				
ANOVA					
	df	SS	MS	F	Significance F
Regression	2	81811.954	40905.98	19.431	0.000
Residual	27	56840.465	2105.202		
Total	29	138652.419			
	Coefficients	Standard Error	t Stat	P-value	
Intercept	34.774	19.098	1.821	0.080	
H MEAN	20.001	3.813	5.245	0.000	
H SUM	-0.014	0.005	-2.801	0.009	

Table 11. Model 2 regression output

Model 2 Regression Statistics					
Multiple R	0.828				
R Square	0.685				
Adjusted R Square	0.662				
Standard Error	40.469				
Observations	30				
ANOVA					
	df	SS	MS	F	Significance F
Regression	2	96149.22	48074.61	29.35	0.000
Residual	27	44219.65	1637.76		
Total	29	140368.87			
	Coefficients	Standard Error	t Stat	P-value	
Intercept	36.774	15.73	2.338	0.027	
H MEAN	21.769	3.286	6.626	0.000	
H SUM	-0.018	0.005	-3.862	0.001	

Table 12. Model 3 regression output

Model 3 Regression Statistics					
Multiple R	0.804				
R Square	0.647				
Adjusted R Square	0.621				
Standard Error	43.989				
Observations	30				
ANOVA					
	df	SS	MS	F	Significance F
Regression	2	95845.528	47922.76	24.766	0.000
Residual	27	52246.098	1935.041		
Total	29	148091.627			
	Coefficients	Standard Error	t Stat	P-value	
Intercept	40.092	18.585	2.157	0.040	
H MEAN	23.52	3.731	6.303	0.000	
H SUM	-0.02	0.005	-3.936	0.001	

Table 13. Model 4 regression output

| Model 4 Regression Statistics					
Multiple R	0.777				
R Square	0.603				
Adjusted R Square	0.574				
Standard Error	46.105				
Observations	30				
ANOVA					
	df	*SS*	*MS*	*F*	*Significance F*
Regression	2	87208.44	43604.22	20.51	0.000
Residual	27	57392.03	2125.63		
Total	29	144600.46			
	Coefficients	*Standard Error*	*t Stat*	*P-value*	
Intercept	39.339	18.724	2.101	0.045	
D CofV	0.054	0.022	2.418	0.023	
H CofV	0.256	0.044	5.864	0.000	
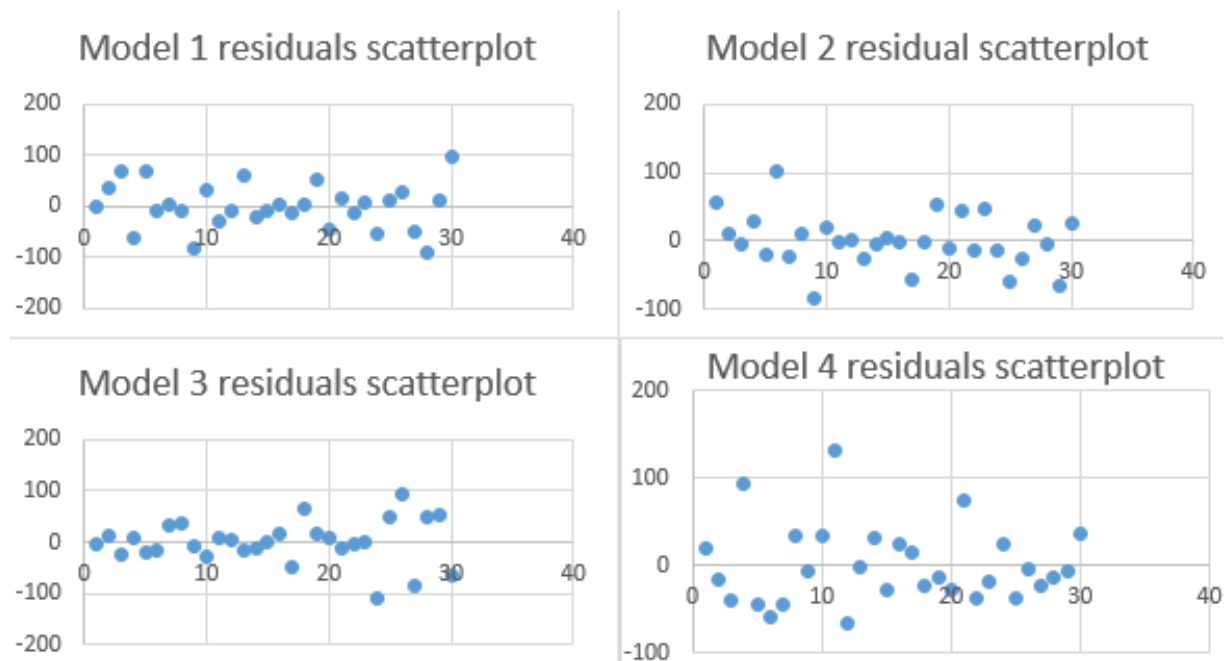
Figure 24. Residual scatter plots for volume models 1 to 4

3.5. Volume Regression Models by Integrated LiDAR Metrics and Pixel Values of Bands From WorldView-3 Imagery

Here the same procedure as above was repeated to come up with regression models but here both the CHM derived metrics and pixel values from the WorldView-3 image bands were all integrated as independent variables. Three regression models were picked as they showed better adjusted R^2s and lower RMSEs. The best adjusted R^2 of 0.70 and with RMSE of 28 m^3 ha^{-1} was obtained from the regression model 5 with Area (A), Height coefficient of variation (H_{cofv}), Height first quartile (H_{1stQ}), Slope (S) and WorldView3 band 6 pixel values ($WV3_{band6pv}$) as independent variables. The second best had adjusted R^2 of 0.6977 and RMSE of 31.93 m^3 ha^{-1} with explanatory variables as mean density (D_{mean}), height coefficient of variation (H_{cofv}) and worldiew3 band 8 pixel values ($WV3_{band8pv}$). The last regression model had adjusted R^2 of 0.692 and RMSE of 35.9 m^3 ha^{-1} and with explanatory variables as height range (H_{range}), height mean (H_{mean}) and worldview3 band 6 pixel values ($WV3_{band6pv}$). Tables 14, 15 and 16 show the regression outputs for these three models.

Table 14. Model 5 regression output

Model 5 Regression Statistics					
Multiple R	0.867				
R Square	0.752				
Adjusted R Square	0.700				
Standard Error	32.325				
Observations	30				
ANOVA					
	df	SS	MS	F	Significance F
Regression	5	76264.35	15252.87	14.5965	0.000
Residual	24	25079.22	1044.968		
Total	29	101343.6			
	Coefficients	Standard Error	t Stat	P-value	
Intercept	294.974	119.821	2.461	0.021	
AREA	-0.206	0.043	-4.705	0.000	
H CofV	-0.401	0.138	-2.892	0.007	
1st Q	39.593	8.862	4.467	0.000	
Slope	-1.393	0.621	-2.240	0.034	
B6_24m	-0.737	0.345	-2.138	0.042	

Table 15. Model 6 regression output

Model 6 Regression Statistics					
Multiple R	0.853				
R Square	0.728				
Adjusted R Square	0.697				
Standard Error	34.299				
Observations	30				
ANOVA					
	df	*SS*	*MS*	*F*	*Significance F*
Regression	3	82278.51	27426.17	23.31288	0.000
Residual	26	30587.4	1176.438		
Total	29	112865.9			
	Coefficients	*Standard Error*	*t Stat*	*P-value*	
Intercept	399.277	102.695	3.887	0.000	
D mean	153.893	62.319	2.469	0.020	
H CofV	0.132	0.038	3.425	0.002	
B8_24m	-1.1943	0.261	-4.571	0.000	

Table 16. Model 7 regression output

Model 7 Regression Statistics					
Multiple R	0.85				
R Square	0.723				
Adjusted R Square	0.691				
Standard Error	38.569				
Observations	30				
ANOVA					
	df	*SS*	*MS*	*F*	*Significance F*
Regression	3	101338.14	33779.38	22.70	0.000
Residual	26	38677.24	1487.58		
Total	29	140015.38			
	Coefficients	*Standard Error*	*t Stat*	*P-value*	
Intercept	418.046	137.311	3.044	0.005	
H RANGE	-5.062	2.247	-2.252	0.032	
H MEAN	13.207	2.696	4.897	0.000	
B6_24m	-1.069	0.426	-2.507	0.018	

Model 5 despite having a superior adjusted R square when tested on the ten test sample plots did perform so well and gave a cross-validated R^2 of 0.17 and had a RMSE of 107.3 m3 ha-1. Model 6 performed better in predictions than model 5 and model 7 as it gave a better cross-validated R^2 of 0.26 and RMSE of 72 m^3 ha-1 for test sample plots. Model 7 performed better than model 5 in terms of predictions and gave cross-validated R^2 of 0.17 and

lowest RMSE of 67 when run on test sample plots. Figures 25, 26 and 27 show scatter plots of predicted volume plotted against observed volume when run on the ten test plots.
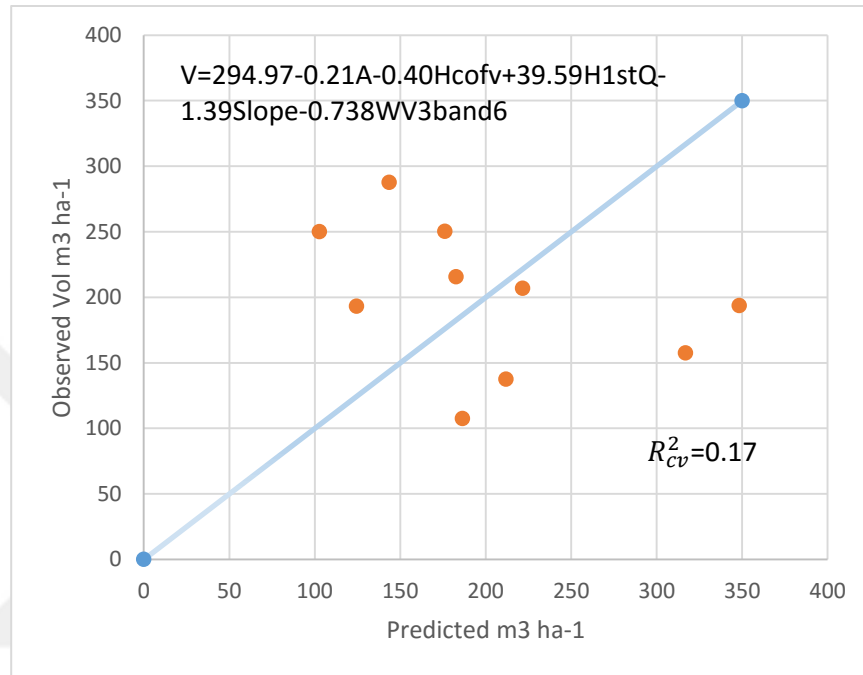

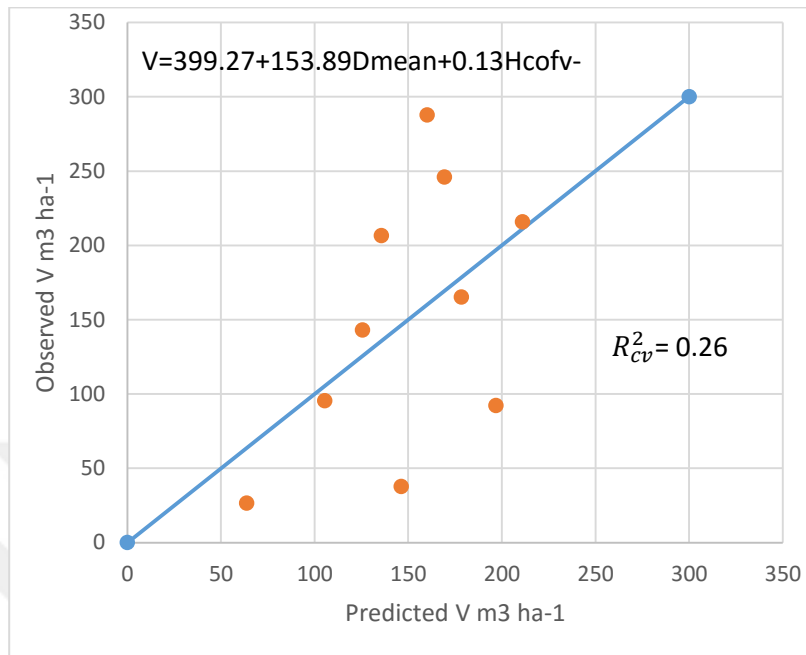Figure 25. Predicted against Observed volume for model 5

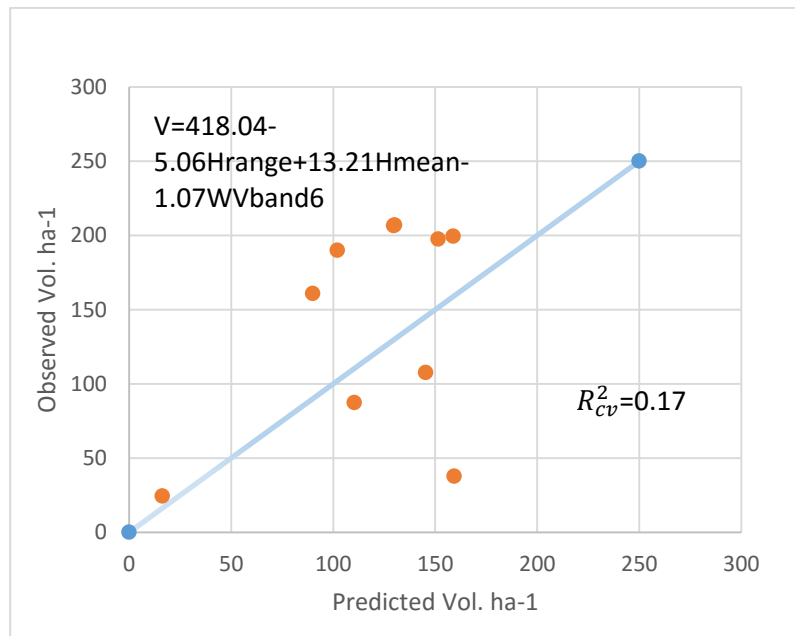Figure 26. Predicted against Observed for model 6

Figure 27. Predicted against observed for mod

4. DISCUSSION

The results of this study have revealed that the proposed practical two-stage procedure by Naesset is robust in investigating forest characteristics. The practical two-stage procedure as proposed by Nasset is done by using field measurements as dependent variables and modelling them against LiDAR metrics as independent variables. The sample plots used to estimate the regression equations in this study were randomly selected. From a total of 40 sample plots, 30 were used to estimate the regression equations while the remaining 10 were used to test the equations/models.

For the sample plot average height, the mean difference between LiDAR derived and observed ground truth values for the ten test sample plots was around 1.5 meters. There was a high Pearson correlation coefficient between the observed average height and predicted average height in the test plots (r=0.83) and a cross-validated coefficient of determination (R_{cv}^2= 0.69). While this result may differ with findings of Nasset (2002) who obtained a mean difference of less than 0.5 meters between average height and dominant height on test plots, sample plots used in this study were not as homogenous as those in Nasset's study in which highly stratified homogenous sample plots were used. In Nasset's study, sample plots were stratified into young forests and mature forests. This might explain the more reason why in Nasset's selected models for average height estimation, maximum height and 90th percentiles were of high significance whilst in this study owing to the heterogeneity in the sample plots, the third quartile of the heights and the mean density were the significant explanatory variables in the selected model for average height. On the other hand, the results of this study are better than that obtained by Mora et al. (2013) who obtained R^2 of 0.76 and RMSE of 1.95 m compared to findings of this study which produced R^2 of 0.83 and RMSE of 1.68. These results are much better than Unger et al. (2014) who obtained R^2 of 0.69 and RMSE of around 5 m though this was for average stand and not for plot and also better than González et al. (2012) who obtained R^2 of 0.786. Figure (28) shows the differences between predicted and observed average plot height when the model was tested on the ten test sample plots.
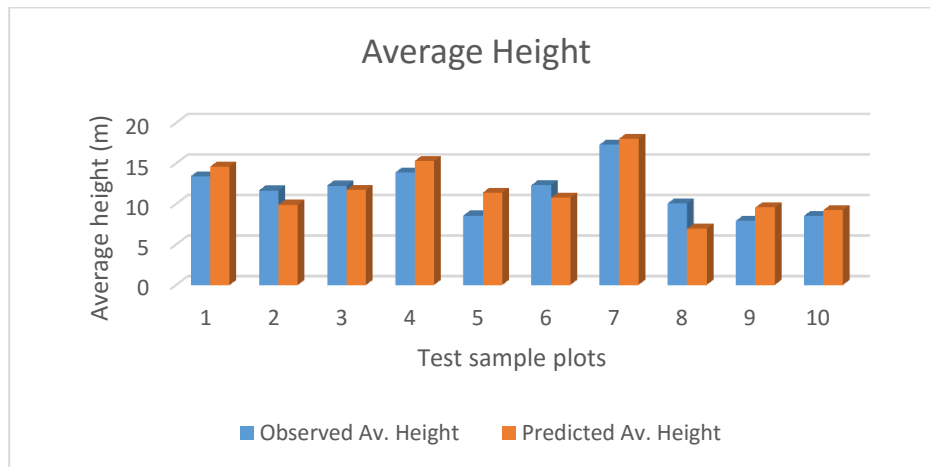
Figure 28. Differences in predicted versus observed average height

For the dominant height, the mean difference between the observed dominant height and the predicted dominant height when the selected model was run on the test plots was around 2 meters with correlation coefficient r of 0.84 and cross-validated R^2_{cv} of 0.72. The regression adjusted R^2 for this model was 0.83 which is exactly the same as that obtained by Nasset and Bjerknes (2001) in their study titled 'estimating tree heights and number of stems in young forest stands using airborne laser scanner data'. However their results were based on 39 sample plots with a homogenous area of 200 m^2. Nasset (2002) obtained R^2s of 0.93, 0.74 and 0.85 for young forests, mature forests in poor sites and mature forests in good sites respectively. The current study had third quartile of heights and 10th percentile of heights as explanatory variables while Nasset et al.'s study had 90th percentile and crown density as explanatory variables. Again this might be attributed to the fact that this study did not have as much homogenous plots as did the former study. However the results of this study for dominant height is less than that found by González et al. (2012) who got R^2 of 0.87. Figure (29) illustrates the differences between predicted and observed dominant heights for the test sample plots.
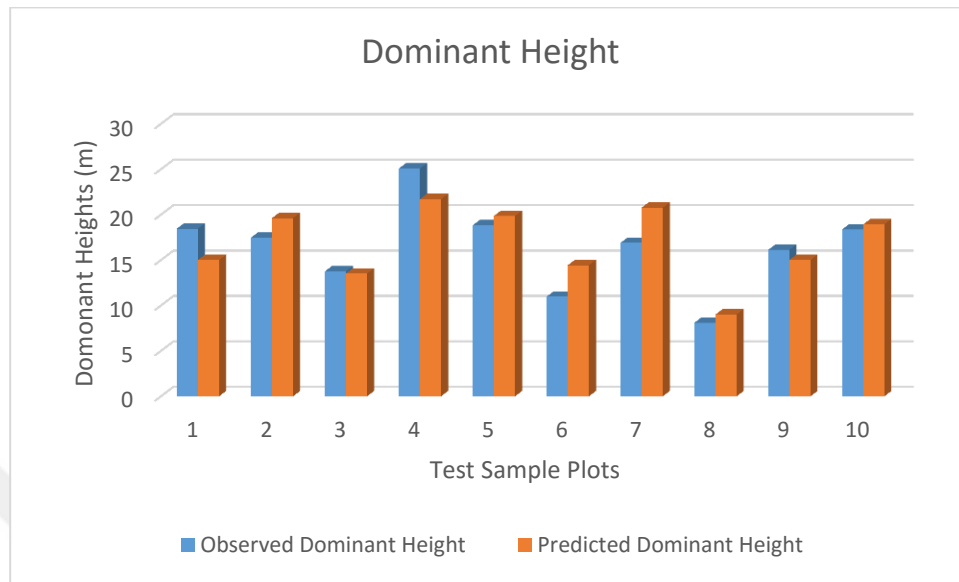
Figure 29. Differences in predicted and observed dominant height

The mean difference of number of stems per hectare between the model predicted in test sample plots and the ground truth data was less than two hundred trees per hectare. Findings of this study are far much better than those of Nasset and Bjerknes (2001) whose regression model had adjusted R^2 of 0.42 while the current study had an adjusted R^2 of 0.73. This might be attributed to that their model had only one explanatory variable, the LiDAR canopy density whilst this study had four explanatory variables in area (A), canopy density standard deviation (D_{std}), 1st quartile of the heights (H_{1stQ}) and the 20th percentile of the heights (H_{20thP}). Also to note in the current study is that the area as explanatory variable played a role as sample plots in this study were not homogenous unlike the study of Nasset and Bjerknes (2001) in which all model training sample plots had an area of 200m^2. Nasset (2002) obtained R^2s of 0.68, 0.65 and 0.50 for young forests, mature forests in poor sites and mature forests in good sites. Unger et al. (2014) obtained R^2 of 0.37 and RMSE of between 94 trees ha^{-1} and 141 trees ha^{-1} as compared to this study in which RMSE for trees per ha was between 109 and 204. However, when the model was tested on test sample plots, there was one case in which number of trees was under estimated by about 900 trees per ha as can be seen in figure (30).
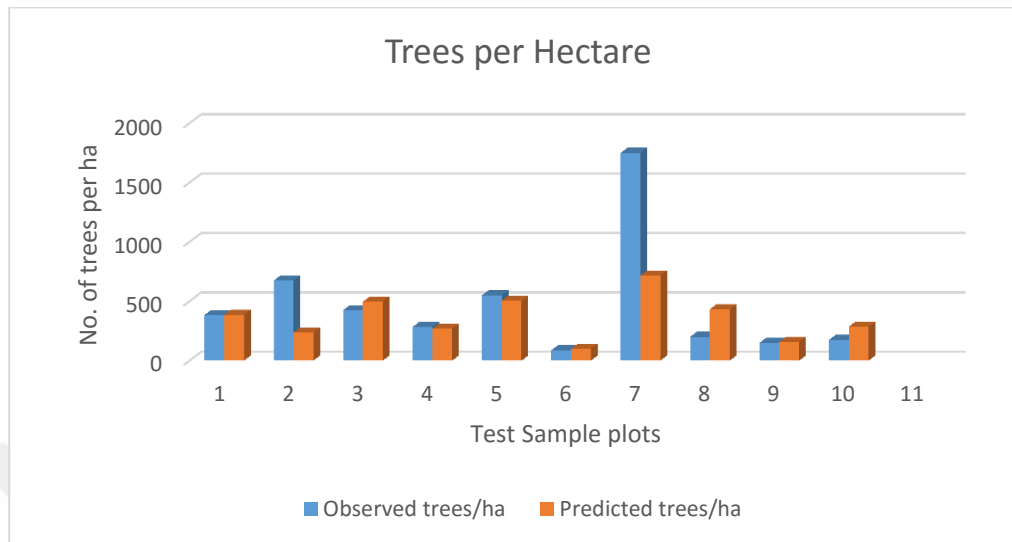
Figure 30. Differences in predicted and observed trees per hectare

As already mentioned in the results, the best regression model for volume per hectare when considering only LiDAR derived metrics had the best adjusted R^2 of 0.66 though the best model if cross validated R^2_{cv} is considered was Model 3 which had adjusted R^2 of 0.62. The lowest RMSE was 38.4 m^3 ha^{-1} and highest 43.7 m^3 ha^{-1}. Kwak et al. (2014) reported lowest adjusted R^2 of 0.51 and highest 0.84 whilst their lowest RMSE was 45.2 m^3 ha^{-1} and highest of 124.5 m^3 ha^{-1} for regression models from canopy height distribution metrics. Nasset (2002) reported R^2 of between 0.80 and 0.93. The findings for the above studies are better than the findings of this study in which the highest adjusted R^2 for volume only went up to 0.66. However, findings of this study do not differ much from the findings of Maack et al. (2016) who reported R^2 of between 0.56 and 0.72. Giannico et al. (2016) also obtained a quiet better R^2 of 0.81 and 23% RMSE. It must be pointed out though that these difference might be attributed to the fact that sample plots used in this study in most cases composed of uneven stands and of various areas unlike in the other studies where same sample plot areas have been used. The explanatory variables for most obtained regression models in this study including the best model selected had the mean height as the major contributor unlike in other studies like for Nasset (2002) and Kwak et al. (2014) in which explanatory variables such as maximum height and/or higher percentiles of heights played a major role. This finding points

to the fact that this current study did not have an even distribution of heights in most sample plots. Also as Maack et al. (2016) pointed out that too much variation between volumes in sample plots, even those of the same area, has a big impact on under estimations and over estimations in volume per hectare. Kwak et al. (2014) in their study of estimating plot volume using LiDAR height and intensity distribution parameters used 30 sample plots of the same age and almost of same height with equal area of 0.05 ha. Nasset (2002) used a lot of sample plots stratified in young and mature stands and thus homogenous. Maack et al. (2016) used a larger area with heterogeneous forests. The findings of this study therefore agrees well with those of Maack et al. (2006) though their study had a very large area and a number of sample plots. They pointed out in their study that their results indicated a biased regression slope that led to overestimation and underestimation of small and large timber volumes, respectively just like was the case in this study. To reduce on this anomaly they divided their dataset into five classes of timber volume (0–200, 200–400,600–800, 800–1200 m^3ha^{-1}). This study however could not divide the dataset due to the fact that the sample size was small.
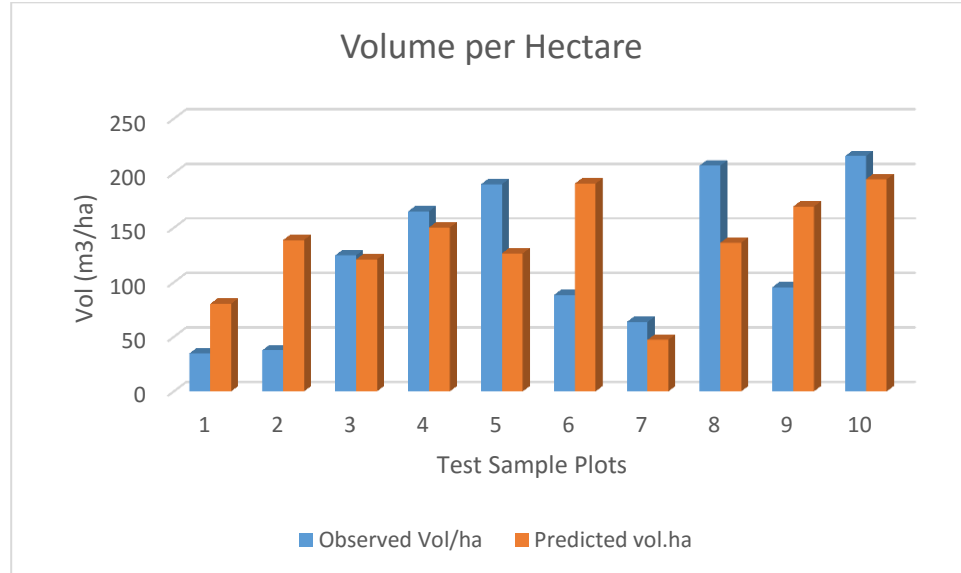

Figure 31. Differences in predicted and observed volume (LiDAR Data alone)

As was expected, models produced from integrated LiDAR metrics and Worldview3 imagery pixel values for the various bands produced better results in terms of adjusted R

squares with the best being between 0.69 and 0.70. Bands 6 and 8, yellow and near infrared 2 respectively proved to be the best bands amongst the eight bands in Worldview3 imagery in volume model regression. However when run on the test sample plots, these models did not perform so well. The model that performed better on test plots though is model 6 which had density mean, height coefficient of variation and Worldview3 band 8 pixel value. This can be attributed to the fact that band 8 (visible near infrared band) plays a key role in modelling volume as the prediction power in terms of cross-validated R^2_{cv} was low for the two models which did not have the band 8 as explanatory variable in them. Mora et al. (2014) obtained a far much better R^2 of 0.94 and very low RMSE of 9.6 m^3 ha^{-1} when they used both LiDAR and high resolution images. On the other hand, the results of this study are similar to those obtained by Chen *et al.* (2011) who got R^2 of 0.72 and a RMSE of 52.59 m^3 ha^{-1} respectively. Also Zald et al. (2016) obtained similar results after integrating high resolution images and LiDAR whose R^2 ranged from 0.42 to 0.69.
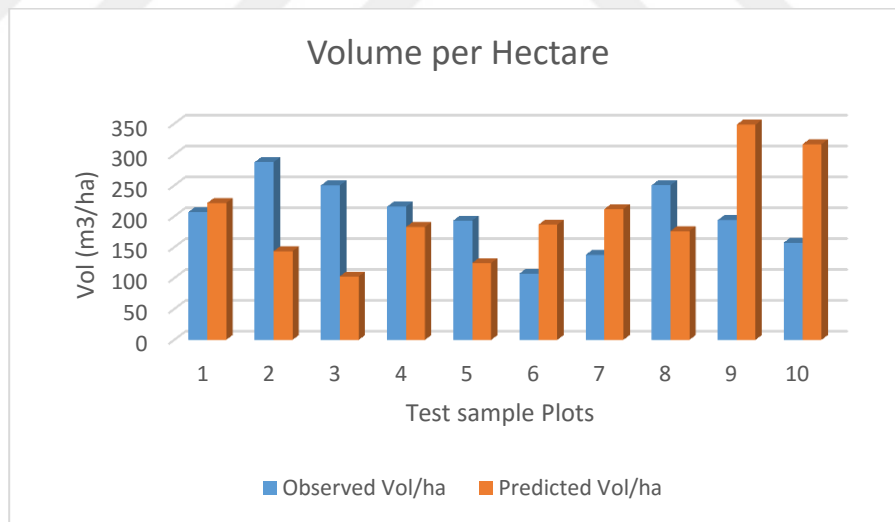
Figure 32. Differences in predicted and observed volume (LiDAR data and WorlfView-3 multispectral bands).

All the models performed well especially if we put into consideration the nature of the study area which is so mountainous and the forest stands are not homogenous. All of models

selected in this study were significant at 0.05 and did their results for the test plots. The proposed procedure is thus credible and can be used even on larger scales.

5. CONCLUSIONS AND SUGGESTIONS

The main objective of this thesis was to develop regression models for estimation of volume and other forest parameters using LiDAR and field data for part of Bergama State Forest Enterprise. This was achieved by developing necessary models in ArcGIS and TreeVis from which metrics were derived and used in multiple regression analysis. Scientifically significant models were produced in SPSS and Microsoft Excel. The best model for average height had adjusted R square of 0.83 with mean density, density coefficient of variation and third quartile height as explanatory variables. Dominant height had the best model with adjusted R square 0.83 and third quartile height and 10th percentile height as explanatory variables. Number of Stems's best model had adjusted R square of 0.73 with area, density standard deviation, first quartile height and 20th percentile height as explanatory variables. For volume, the best model from LiDAR metrics alone gave an adjusted R square of 0.66 with explanatory variables being the plot mean height and the sum of all heights in a given plot. When LiDAR metrics were integrated with pixel values of bands from WorldView-3, the best model produced had R square of 0.70 with explanatory variables being area, height coefficient of variation, first quartile of heights, slope and Worldview-3 band 6 pixel values. Over all, the mean height proved to be the major predictor variable from LiDAR metrics while bands 6 and 8 were the main predictor variables from WorldView-3's bands.

The results of this master thesis research therefore confirms, just like other published studies, that LiDAR data has a strong potential to provide relatively accurate information on volume per hectare and can offer a good estimation of average tree heights and dominant heights. Also that the integration of LiDAR metrics and pixel values from WorldView-3 can improve the model performance as was witnessed by a higher adjusted R square after using integrated data.

Listed here under are some recommendations coming after the works of this master thesis:

❖ Other studies need to be conducted around the same area but using other LiDAR systems such as Optech and with different flight heights and using well classified and ground verified cloud points.

❖ In this study, different sample plot sizes were used which might have affected the prediction accuracy. It is therefore highly recommended that another study be done around the same area but using a uniform sample plot area to see if this has an effect as reported in other studies.

❖ The latest high resolution imagery, WorldView-3, can be explored further and would be tried using other bands such as the short wave near infrared (SWIR) and LiDAR height metrics.

❖ Also similar studies should be conducted in different and uniform forest stands and with different forest stand types (species).

❖ Diameter at breast height is the other parameter that can be explored especially because dense LiDAR data is capable of delineating individual trees. The crown diameter can be related to the diameter at breast height.

❖ Lastly but not the least, the major challenge faced in this study was that of normalizing DTM and DSM when using GIS. A proper standalone script in python should be developed for production of these models so not to incur negatives in the CHM.

6. REFERENCES

Akay, A. E. , Hakan, O., Ismail, R.K., and Kazuhiro, A., 2009. Using LiDAR technology in forestry activities, Environment Monitoring Assessment, 151, 117–125.

Aldred, A. and Bonner, M., 1985. Application of airborne lasers to forest surveys. Canadian Forestry Service, Petawawa National Forestry Centre, Information Report PI-X-51, 62.

Apostol, B., Petrila, M., Lorent, A., Gancz, V. and Cret, A., 2010. Potential use of airborne LiDAR technology by the integration of remote sensing and terrestrial datasets for forests assessment and mapping in Romania. Proceedings of the Biennial International Symposium, Forest and Sustainable Development, Brasov, Romania, 15-16th October 2010 Brasov: Transilvania University Press, 513-518

Arp, H., Griesbach, J. and Burns, J. 1982. Mapping in tropical forests: a new approach using the laser APR. Photogrammetric Engineering and Remote Sensing, 48, 91–100.

Asner, G. P., and Martin, R. E., 2009. Airborne spectranomics: Mapping canopy chemical and taxonomic diversity in tropical forests. Frontiers in Ecology and the Environment, 7, 5, 269–276.

Astola, H., Bounsaythip, C., Ahola, J., Häme, T., Parmes, E., Sirro, L. and Veikkanen, B., 2004. HIGHFOREST – forest parameter estimation from high resolution remote sensing data, Technical Research Centre of Finland, Information Technology, Information Systems, 259–264.

Ateşoğlu, A., 2009. Using different satellite images to develop regression models for forest stand parameters (A case study for Bartin-Mugada), PhD thesis, Bartin University, Graduate School of Natural and Applied sciences, Bartin.

Axelsson, P., 1999. Processing of laser scanner data–algorithms and applications. ISPRS Journal of Photogrammetry and Remote Sensing, 54, 138–47.

Aydın, M., 2014. Technical Report on the possibility og using LiDAR in forest management planning, General Direstorate of Forestry, Ankara, 10 pages.

Azita, A. Z., Shiba, M. and Jemali, J. N., 2015. Accuracy of LiDAR-based tree height estimation and crown recognition in a subtropical evergreen broad-leaved forest in Okinawa, Japan. Forest Systems 24, 1, 11.

Cavalli, M., Tarolli, P., Marchi, L. and Fontana, G.D. 2008. The effectiveness of airborne LiDAR data in the Hohenthal et al. 803 recognition of channel-bed morphology. Catena 73, 249–260.

Chen, Q., P. Gong, D. Baldocchi, and Tian, Y. Q., 2007. Estimating Basal Area and Stem Volume for Individual Trees from LiDAR Data. Photogrammetric Engineering & Remote Sensing, 73, 1355–1365.

Chen, G., Hay, G.J. and St-Onge, B.A. 2012. GEOBIA framework to estimate forest parameters from lidar transects, Quickbird imagery and machine learning: A case study in Quebec, Canada. Int. J. Appl. Earth Obs. Geoinf, 15, 28–37.

Clark, M. L., Roberts, D. A., and Clark, D. B., 2005. Hyperspectral discrimination of tropical rain forest tree species at leaf to crown scales. Remote Sensing of Environment, 96, 3–4, 375–398.

Çil, B., 2015. Bazı Meşcere Parametrelerinin Farklı Uydu Görüntüleri Yardımıyla Tahmin Edilmesi: Kelkit ve İğdir Planlama Birimi Örneği, Yüksek Lisans Tezi, Karadeniz Teknik Üniversitesi Fen Bilimleri Enstitüsü, Trabzon.

Çil, B., Karahalil, U. ve Karslı, F., 2015. Uzaktan Algılama Verileri Yardımıyla Bazı Meşcere Parametrelerinin Tahmin Edilmesi:Kütahya/Tetik Planlama Birimi Örneği, TUFUAB VIII. Teknik Sempozyumu, Mayıs, Konya, Bildiriler Kitabı, 170-176.

Davis, L.S., Johnson, K.N., Bettinger, P.S. and Howard, T.S., 2001. Forest Management. 2001. Davis, Johnson, Bettinger, and Howard. 4th edition. McGrawHill, New York, NY.

Dubayah, R., and J. B. Drake., 2000. Lidar Remote Sensing for Forestry. Journal of Forestry 98, 44–46.

Ellis, P., Griscom, B., Walker, W., Gonçalves, F. and Cormier, T., 2016. Mapping selective logging impacts in Borneo with GPS and airborne lidar. Forest Ecology and Management, 365, 184–196.

Esri, 2011. White paper; Lidar Analysis in ArcGIS® 10 for Forestry Applications.

Giannico, V., Lafortezza, R., John, R., Sanesi, G., Pesola, L. and Chen, J., 2016. Estimating Stand Volume and Above-Ground Biomass of Urban Forests Using LiDAR. Remote Sens, 8, 339.

GDF, 2008. Yenisakran Forest Management Plan, General Directorate of Forestry, 286, Ankara.

González, D., Becker, J., Torres, E., Albistur, J., Escudero, M., Fuentes, R., Hinostroza, H. and Donoso, F., 2008. Proceedings of SilviLaser 2008, 8th international conference on LiDAR applications in forest assessment and inventory, Heriot-Watt University, Edinburgh, UK, 17-19 September, 2008 Bournemouth: SilviLaser 2008 Organizing Committee, 437-445.

González-Ferreiro, E., Diéguez-Aranda, U. and Miranda, D., 2012. Estimation of stand Variables in Pinus radiata D. Don plantations using different LIDAR pulse densities. Forestry, 85,2, 281-292.

Guenther G.C., 2007. Airborne lidar bathymetry. In: Maune DF (ed.) Digital Elevation Model Technologies and Applications: The DEM User's Manual, second edition. Bethesda, MD: American Society for Photogrammetry and Remote Sensing, 253–320.

Günlü, A., Ercanlı, I., Başkent, E.Z. and Şenyurt, M., 2013. Predicting stand volume using Quickbird and Landsat 7 ETM+ satellite images for stands of oriental beech (*Fagus orientalis* Lipsky): a case study in Ayancık-Göldağ, SDU Faculty of Forestry Journal, 14: 24-30.

Günlü, A., Başkent, E.Z., Ercanlı, İ. and Şenyurt, M., 2015. Estimating Dominant Height Using Landsat 7 ETM Satellite Image in Pure Oriental Beech Stands in Göldağ, Sinop, The 10th International Beech Symposium, Abstract Book, 79, 1-6 September, Kastamonu, Turkey.

Holmstrom, C., Egan, S., Franks, S., McCloy, S. and Kjelleberg, S., 2002. Antifouling activities expressed by marine surface associates Pseudoalteromonas species. FEMS Microbiol Ecol 41, 47–58.

Huang, M., and Asner, G. P., 2009. Long-term loss and recovery following selective logging in Amazon forests. San Francisco, CA: American Geophysical Union.

Immitze, M., Stepper, C., Böck, S., Straub, C. and Atzberger, C., 2016. Use of WorldView-2 stereo imagery and National Forest Inventory data for wall-to-wall mapping of growing stock. Forest Ecology and Management, 359, 232–246.

İnan, M., 2004. Detecting the presence of forests using remote sensing data, PhD thesis, Istanbul University, Graduate School of Natural and Applied sciences, Istanbul.

JiLi, L., BaoXin, H. and Noland, T. L., 2013. Classification of tree species based on structural features derived from high density LiDAR data. Agricultural and Forest Meteorology, 171-172, 104-114.

Kajisa, T., Murakami, T., Mizoue, N., Top, N. and Yoshida, S., 2009. Object-based forest biomass estimation using Landsat ETM+ in Kampong Thom Province, Cambodia. J. For. Res, 14, 4, 203–211.

Kayı, A., Eroğan, M. and Eker, O., 2015. Results of LIDAR Test Performed by Optech-HA 500 and REIGL LMS-Q 1560, Journal of Mapping, General Command of Mapping, No: 153.

Khorrami, R., 2004. Evaluating ETM+ data to assess the standing tree volume on *Fagus orientalis* stands (a case study of Sangdeh forests). M.Sc. dissertation, Faculty of Natural Resources, University of Tehran, Iran, 80.

Krabill, W.B., Collings, J.G., Swift, R.N. and Butler, M.L., 1980. Airborne laser topographic mapping results from Initial Joint NASA/U.S. Army Corps of Engineers Experiment. NASA.

Krabill, W.B., Collins, J.G., Link, L.E., Swift, R.N., and Butler, M.L., 1984. Airborne laser topographic mapping results. Photogrammetric Engineering & Remote Sensing 50, 6: 685-694.

Kutner, M., C. Nachtsheim, and J. Neter, eds. 2004. Applied Linear Regression Models. 4th Ed.

Kvålseth, T. O. 1985. "Cautionary Note about R2." American Statistician 39, 279–285.

Laurin, G.V., Chen, Q., Lindsell, J.A., Coomes, D.A., Del Frate, F.,Guerriero, L., Pirotti, F. and Valentini, R., 2014. Above ground biomass estimation in an African tropical forest with LiDAR and hyperspectral data. ISPRS Journal of Photogrammetry and Remote Sensing, 89, 49–58.

Leckie, D. G., 1990. Advances in Remote Sensing Technologies for Forest Surveys and Management. Canadian Journal of Forest Research, 20, 464–483.

Kwak, D.A., Lee, W.K., Cui, G., Cho, H.K., Jeon, S.W. and Lee, S.H., 2014. Estimating plot volume using lidar height and intensity distributional parameters. International Journal of Remote Sensing, 35, 13, 4601–4629.

Lefsky, M. A., Harding, D., Cohen, W. B., Parker, G. and Shugart, H. H., 1999. Surface lidar remote sensing of basal area and biomass in deciduous forests of eastern Maryland, USA. Remote Sensing of Environment, 67, 83– 98.

Lefsky, M., Cohen, W. and Spies, T., 2001a. An evaluation of alternate remote sensing products for forest inventory, monitoring, and mapping of Douglas-fir forests in western Oregon. Canadian Journal of Forest Research, 31, 78–87.

Lefsky, M.A., Harding, D., Cohen, W.B., Parker, G. and Shugart, H.H. 1999a: Surface LiDAR remote sensing of basal area and biomass in deciduous forests of Eastern Maryland, USA. Remote Sensing of Environment, 67, 83–98.

Lim, K., Treitz, P., Wulder, M., St-Onge, B. and Flood, M., 2003. LiDAR remote sensing of forest structure. *Progress in Physical Geography* 27, 1, 88–106.

Lopez, F., Ek, A.R. and Bauer, M.E., 2001. Estimation and mapping of forest stand density, volume, and cover type using the k-nearest neighbors method. Remote Sensing of Environment 77, 251 – 274.

Maack, J., Lingenfelder, M., Weinacker, H. and Koch, B., 2016. Modelling the standing timber volume of Baden-Württemberg—a large-scale approach using a fusion of Landsat, airborne LiDAR and National Forest Inventory data. International Journal of Applied Earth Observation and Geoinformation, 49, 107–116.

MacLean, G.A. and Krabill, W.B., 1986. Gross merchantable timber volume estimation using an airborne LiDAR system. Canadian Journal of Remote Sensing, 12, 7–18.

MacLean, G.A. and Martin, G.L., 1984. Merchantable timber volume estimation using cross-sectional photogrammetric and densitometric methods. Canadian Journal of Forest Research, 14, 803–10.

Magnussen, S. and Boudewyn, P., 1998. Derivations of stand heights from airborne laser scanner data with canopy-based quantile estimators. Canadian Journal of Forest Research, 28, 1016–31.

Magnussen, S., Eggermont, P. and LaRiccia, V.N., 1999. Recovering tree heights from airborne laser scanner data. Forest Science, 45, 407–22.

Maiman TH. 1960. Stimulated optical radiation in ruby. Nature, 187, 493–494.

Makela, H. and Pekkarinen, A., 2004. Estimation of forest stand volumes by Landsat TM imagery and stand–level field–inventory data. Forest Ecology and Management, 196, 245–255.

Maltamo, M., J. Hyyppä, and J. Malinen. 2006. "A Comparative Study of the Use of Laser Scanner Data and Field Measurements in the Prediction of Crown Height in Boreal Forests." Management. Canadian Journal of Forest Research 20, 464–483.

Marks, K. and Batesm P., 2000. Integration of high-resolution topographic data with floodplain flow models. Hydrological Processes, 14, 2109–2122.

Means, J. E., S. A. Acker, B. J. Fitt, M. Renslow, L. Emerson, and Hendrix, C. J., 2000. Predicting Forest Stand Characteristics with Airborne Scanning LiDAR. Photogrammetry Engineering and Remote Sensing 66, 1367–1371.

Means, J. E., Acker, S. A., Harding, D. J., Blair, J. B., Lefsky, M. A., Cohen, W. B., Harmon, M. E. and W. A. McKee. 1999. Use of Large Footprint Scanning Airborne LiDAR to Estimate Forest Stand Characteristics in the Western Cascades of Oregon. Remote Sensing of Environment, 67, 298–308.

Mısır, M., 2013. Estimating forest stand parameters using Landsat 7 ETM satellite image. Antalya: Forest sector planning, 50th international symposium, November, Antalya, Proceedings Book: 529-537.

Mohammadi, J., Shattaee, S., Yaghmaee, F. and Mahiny A.S., 2006. Modelling forest stand volume and tree density using Landsat ETM+ data. International Journal of Remote Sensing, 31, 11, 2959–2975.

Mora, B., Wulder, M. A., White, J. C. and Hobart, G., 2013. Modeling Stand Height, Volume, and Biomass from Very High Spatial Resolution Satellite Imagery and Samples of Airborne LiDAR. Remote Sens, 5, 2308-2326.

Naseri, F. 2003. Classifying the forest plant types and estimating their quantitative properties using satellite data from forest located at dry and semidry areas. PH.D. thesis on forestry. Tehran University, P 202.

Naesset, E., 2002. Predicting forest stand characteristics with airborne scanning laserusing a practical two-stage procedure and field data. Remote Sensing of Environment, 80, 88–99.

Naesset, E. 1997a. Determination of mean tree height of forest stands using airborne laser scanner data. ISPRS J. Phofogramm. Remote Sens, 52, 49-56.

Naesset, E. and Bjerknes, K. -O. 2001. Estimating tree heights and number of stems in young forest stands using airborne laser scanner data. Remote Sensing of Environment, 78, 328–340.

Naesset, E. and Økland, T., 2001. Estimating tree height and tree crown properties using airborne scanning laser in a boreal nature reserve. Remote Sensing of Environment, 79, 105–115.

Nelson, R., 1997. Modeling forest canopy heights: The effects of canopy shape. Remote Sensing of Environment, 60, 327–34.

Nelson, R., Krabill, W. and Maclean G., 1984. Determining forest canopy characteristics using airborne lidar data. Remote Sensing of Environment, 15, 201–212.

Nilsson, M., 1996. Estimation of tree heights and stand volume using an airborne lidar system. Remote Sensing and Environment, 56, l-7.

O'Brien. R. M. 2007. A Caution Regarding Rules of Thumb for Variance Inflation Factors.

Özdemir, İ. and Mert, A., 2007. Estimating forest volume of red pine using Quickbird satellite image. Süleyman Demirel University Faculty of Forestry Journal, Series A, No.: 2, ISSN: 1302-7085, 107-118.

Özdemir, İ. and Karnieli, A., 2011. Predicting forest structural parameters using the image texture derived from WorldView-2 multispectral imagery in a dryland forest, Israel, International Journal of Applied Earth Observation and Geoinformation, 13, 701–710.

Özdemir, İ., 2013. Estimation of forest stand parameters using airborne LIDAR data. SDÜ Orman Fakültesi Dergisi, SDU Faculty of Forestry Journal, 14, 31-39.

Özkan, U. Y., 2003. Estimation of forest parameters using satellite images and using such their use I forest management, Master thesis, Istanbul University, Graduate School of Natural and Applied sciences, Istanbul.

Parker, R. C. and Glass, P. A., 2004. High- Versus Low-Density LiDAR in a Double-Sample Forest Inventory. Southern Journal of Applied Forestry, 28, 205–210.

Price WF and Uren J. 1989: Laser Surveying. London: Van Nostrand Reinhold (International) Quality and Quantity, 41, 673–690.

Qiu, F. and Zhou, Y., 2015. Fusion of high spatial resolution WorldView-2 imagery and LiDAR pseudo-waveform for object-based image analysis. ISPRS Journal of Photogrammetry and Remote Sensing, 101, 221–232.

Reese, H., Nilsson, M., Sandström, P. and Olsson, H., 2002. Applications using estimates of forest parameters derived from satellite and forest inventory data. Comput. Electron. Agric, 37, 37–55. http://dx.doi.org/10.1016/S0168-1699(02)00118-7.

Saito, Y., Saito, R., Kawahara, T.D., Nomura, A. and Takeda, S., 2000. Development and performance characteristics of laser-induced fluorescence imaging LiDAR for forestry applications. Forest Ecology and Management, 128, 129–37.

SAS. 2006. SAS User Guide. Cary, NC: SAS Institute Inc.

Schreier H, Lougheed J, Tucker C, and Leckie D., 1985. Automated measurement of terrain reflection and height variations using an airborne infrared laser system. International Journal of Remote Sensing, 6, 101–113.

Şenyurt, M., Günlü, A., Ercanlı, İ. and Yılmaz, C., 2013. Using Landast 8 satelite image to estimate forest stand parameters for Karşıkent state forest enterprise, Forest sector planning 50th international symposium, November, Antalya, Proceedings Book: 497-503.

Shang, X., Chazette, P., Totems, J., Dieudonné, E., Hamonou, E., Duflot, V., Strasberg, D., Flores, O., Fournel, J. and Tulet, P., 2016. Tropical Forests of Réunion Island Classified from Airborne Full-Waveform LiDAR Measurements. Remote Sens, 8, 43.

Shataee, S., 2013. Forest attributes estimation using aerial laser scanner and TM data. Forest Systems, 22, 3, 484-496.

Smreček, R., and Z. Danihelová. 2013. "Forest Stand Height Determination from Low Point Density Airborne Laser Scanning Data in Roznava Forest Enterprise Zone (Slovakia)." iForest – Biogeosciences and Forestry, 6, 48–54.

Smullins, L.D. and Fiocco, G., 1962. Optical echoes from the Moon. Nature 194, 1267.

Solodukhin, V., Zuko,v A. and Mazugin, I., 1977. Possibilities of laser aerial photography for forest profiling. Lesnoe Khozyaisto (Forest Management), 10, 53–58.

Straub, C., Tian, J., Seitz, R. and Reinartz, P., 2013. Assessment of Cartosat-1 And WorldView-2 stereo imagery in combination with a LiDAR-DTM for timber volume estimation in a highly structured forest in Germany. Forestry, 86, 463–473.

Tomppo, E., Olsson, H., Ståhl, G., Nilsson, M., Hagner, O. and Katila, M., 2008. Combining national forest inventory field plots and remote sensing data for forest databases. Remote Sens. Environ, 112, 1982–1999.

Tveite, B., 1977. Site index curves for Norway spruce (Picea abies (L.) Karst.). Reports of the Norwegian Institute for Forest Research, 33, 1 – 84.

Unger, D., Hung, I-K., Brooks, R. E. and Williams, H. M., 2014. Estimating Number of Trees, Tree Height and Crown Width using Lidar Data. *Faculty Publications*. Paper 31. http://scholarworks.sfasu.edu/spatialsci/31.

URL-1, http://www.fao.org/docrep/w7714e/w7714e05.htm. 20th April, 2016.

URL-2, https://www.digitalglobe.com/resources/white-papers. 5TH March 2016.

URL-3, http://www.digitalglobeblog.com/2014/09/03/revealing-the-hidden-world-with shortwave   infrared-swir-imagery/. 30th May, 2016.

URL-4,http://gis.stackexchange.com/questions/136075/fill-in-nodata-gaps-in-raster-using arcgis- for-desktop. 10th March, 2016.

Wehr, A. and Lohr, U., 1999. Airborne laser scanning – an introduction and overview. *ISPRS* Journal of Photogrammetry and Remote Sensing, 54, 68–82.

Young, M. 1986. Optics and lasers: including fibers and optical waveguides. Berlin: Springer Verlag.

Zawawi, A. A., Shiba, M. and Jemali, N. J. N., 2015. Accuracy of LiDAR-based tree height estimation and crown recognition in a subtropical evergreen broad-leaved forest in Okinawa, Japan. Forest Systems, 24, 1, e002, 11.

Zald, H.S.J., Wulder, M.A., White, J.C., Hilker, T., Hermosilla, T., Hobart, G. W. and Coops, N.C., 2016. Integrating Landsat pixel composites and change metrics with LiDAR plotsto predictively map forest structure and aboveground biomass in Saskatchewan, Canada. Remote Sensing of Environment, 176, 188–20.

Ziegler, M., Konrad, H., Hofrichter, J., Wimmer, A., Ruppert, G., Schardt, M., and Hyyppa¨, J., 2000. Assessment of forest attributes and single-tree segmentation by means of laser scanning. Proceedings of the International Society for Optical Engineering, 4035, 73– 84.

Curriculum Vitae

Kennedy KANJA was born on 12th October 1984 in Samfya District of Zambia. After completing primary and later secondary education, KANJA enrolled for Bachelor of Science degree in School of Natural Resources of the Copperbelt University in Kitwe, Zambia where he graduated as one of the top three students in Wood Science and Technology. He worked as Trainee inspector for Zambia Bureau of Standards and later as Tutor at City University College of Science and Technology before getting a scholarship to study for his Master of Science degree in Forestry Engineering at Karadeniz Technical University in Turkey. KANJA speaks English language, Turkish language as well as a number of local languages of Zambia.